# African Journal of Engineering Research and Innovation

AJERI Vol 2. No. 3. 2024

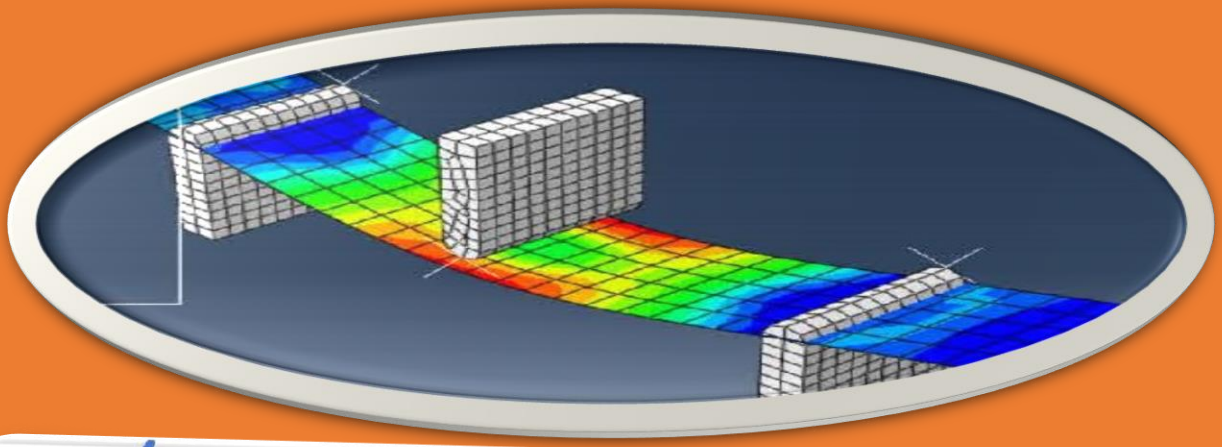

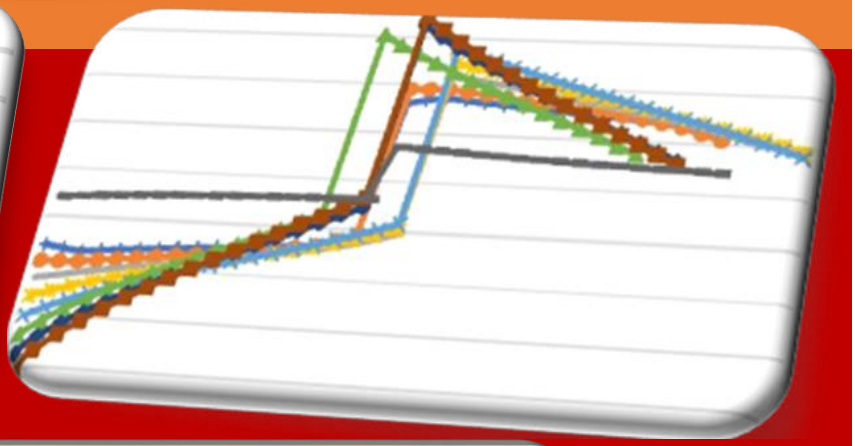

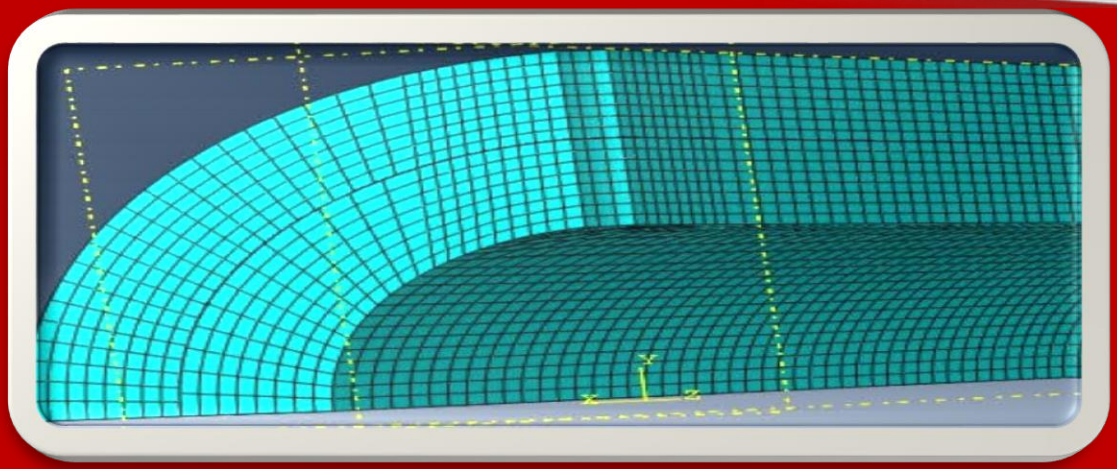

## The Institution of Engineers of Kenya

ISSN: 2957- 7780

In partnership with



ISSN: 2957- 7780

# AJERI

## *African Journal of Engineering in Research and Innovation*

ISSN: 2957- 7780 Volume 2. No 3. 2024

Published by:

The *Institution of Engineers of Kenya*

P.O Box 41346- 00100

Nairobi Kenya

Tel: +254 (20) 2729326, 0721 729363, (020) 2716922

Email: editor@iekenya.org

Website: www.iekenya.org

**IEK**

**African Journal of Engineering Research and Innovation (AJERI),** is published by **The *Institution of Engineers of Kenya*,** IEK, as an international forum for publication of high-quality papers in all areas of Engineering

 ISSN: 2957- 7780

**CONTENTS** **Pages**

**Techno-Economic Modelling and Simulation of Offshore Wind Farm for Lamu Port and its Environs..... 6**

C. B. Owino, G. G. Kidegho, M. J. Saulo

**Enhancing Geothermal Drilling Efficiency: Kenyan Bentonite as a Versatile Drilling Mud ....** Error! Bookmark not defined.**3**

P. M. Weramwanja, G. Rading, T. Ochuku, J. Kihiu, J. Borode

**A Unified Symbol Error Rate (SER) Expression for Equal Gain Combining (EGC) and Maximum Ratio Combining (MRC) over Correlated Nakagami-m Fading Channels ..... 377**

E. Omosa, P. O. Akuon, and V. O. Kalecha

**Climate Change and Water Systems Management in Kenya..... 57**

O. M. Ambani, E. K. Biamah, C. Kipkemoi

**The Place of Forensic Structural Audits and Structural Integrity Evaluations in Resolution of Collapsing of Buildings..... 711**

S. Murianka , J. Ireri

 ISSN: 2957- 7780

# Techno-Economic Modelling and Simulation of Offshore Wind Farm for Lamu Port and its Environs

C. B. Owino*, G. G. Kidegho, M. J. Saulo

Technical University of Mombasa, P.O. Box 90420-80100 Mombasa, Kenya.

*Corresponding author: benardchiaw@gmail.com

***Article History***
*Submission Date: 28th June 2023*
*Acceptance Date: 20th August 2023*
*Publication Date: 30th September 2024*

## Abstract

This paper presents the dynamic modelling and simulation of offshore wind energy (OWE) potential in Lamu of Coastal Kenya. The main area of concern in Coastal Kenya is the Lamu Port and its environs as the main energy consumers. There are the already three operational berths among the thirty two proposed berths that call for more resources and power demand currently based on future projections. The modelling and simulation process considered the wind speed data acquired from Kenya Meteorological Department (Kenya Met.). For the dynamic modelling and simulation, Virtual Wind Farms (VWFs) were developed using different average monthly wind speed data for different years and average power demand projections. These were to be realized for annual-based business models by application software tool called Hybrid Optimization Model for Energy Renewable (HOMER). From the models, optimization results and sensitivity analysis results were achieved in terms of engineering results such as peak daily power production and annual energy output (AEO) as well as the economic indicators such as Pay-Back Period (PBP), Internal Rate of Return (IRR), Return on Investment (ROI), Net Present Value (NPV) and Levelized Cost of Energy (LCOE) to serve any interested investor and the government as well investors. In this paper presents sets of results for the two different power demand projections modelled and simulated using the same set of the adjusted monthly average wind speed data. The proposed 2030 offshore wind farm, expected to meet the 50 MW peak daily average demand, realized the following set results: daily peak generation of 50,160 kW, AEO of 266,204,237 kWh, NPV of $ 1,088,225.00, LCOE of $ 20.47/MWh, PBP of 3.36 years, IRR of 6.13% and ROI of 77.87%. The proposed 2050 offshore wind farm, expected to meet the 200 MW peak daily average demand, realized the following set of results: daily peak generation of 200,640 kW, AEO of 1,064,816,947 kWh, NPV of $ 285,447.70, LCOE of $ 5.37/MWh, PBP of 3.19 years, IRR of 4.05% and ROI of 76.95%.

**Key abbreviations:** OWE, OWF, VWF, HOMER, AEO, PBP, IRR, NPV, LCOE, ROI

 ISSN: 2957- 7780

## 1. Introduction

According to Elsner report of 2019, a number of researches were conducted by World Bank's funded "Energy Sector Management Assistance Program (ESMAP) (Nyambegera, 2021). The sector carried out estimation research on the potentials of offshore wind energy (OWE) in Kenya. The projections of such researches were that Kenya has offshore wind energy potential of 9.35GW for bottom fixed foundation and 81.72GW for floating foundation wind farms (Nyambegera, 2021).

In spite of industrial development in coastal region of Kenya with Lamu having initiated mega economic project involving the establishment of 32 berths – three being currently operational (LAPSSET) project (LAPSSET Corridor Development Authority [LCDA], 2016), However, there existed no energy generation systems from naturally available ocean energy sources. The energy generation from ocean natural sources would be realized by establishing an offshore wind farm that could be made feasible for such projections to boost their energy requirements.

To establish techno-economic feasibility framework that can inform both the government and investors' interests in the exploitation of naturally available ocean energy sources, the work presented on this paper, therefore seek to perform a comprehensive techno-economic feasibility and analysis from a virtual wind farm (VWF) model for the generation project for Lamu port and its environs. This port is within Lamu County (LAMU COUNTY INTEGRATED DEVELOPMENT PLAN September 2018 County Integrated Development Plan , 2022).

The load profile data used in modelling and simulation here, were obtained from Kenya Power and Lighting Company (KPLC) Limited. According to KPLC, Lamu had power projections based on development of the proposed berths for Visions 2030 and 2050. From the data obtained, the KPLC has a projection of average peak daily power demand of 50 MW as per Vision 2030 and 200 MW as per Vision 2050. From the 2021 - 2031 Least Cost Development Plan (LCDP), the Lamu power demand forecast factors are envisioned for various projects in Kenya under Vision 2030 (REPUBLIC OF KENYA - Ministry of Energy, 2021). This forecast would range between 10 MW as the base load to 40 MW. In comparison to Vision 2030 projection, 50 MW was therefore considered as daily average peak demand.

The key wind parameters that would be focused on for the dynamic modelling and simulation include: the wind speed, load profile and wind turbine's specifications. These parameters play a very vital role when determining the power output, and hence the energy generated by the wind turbine at different altitude (Khajah & Philbin, 2022). The wind data used for the work presented here was collected from Kenya Meteorological department before the necessary adjustments were done using mathematical models

 ISSN: 2957- 7780

designed here. The wind speed data collection at Lamu Meteorological Station were done at an altitude of 10 m. Adjustments would therefore be necessary to conform with a standard wind turbine's hub height of 50 m. Based on the objective to achieved the optimization and sensitivity analysis results, HOMER simulation tool was considered and used.

The technical analysis for the offshore wind farm (OWF) simulation model encompasses the wind resource distribution in terms of altitude and time variation (Maandal & Danao, 2021), (Maandal & Danao, 2021). The Power law method would be possibly be used in determining the wind speed distribution with variation in altitude (Derakhshan et al., 2018) while Wei-bull distribution method (not considered in the work presented here) is normally used for determining wind speed distribution with variations based on time (Maandal & Danao, 2021), (Shu & Jesson, 2021). Other technical analysis parameters that would be suitable for use in the designed model, presented on this paper include the wind turbine and specifications, the energy storage system and the power converters (Maandal & Danao, 2021).

The economic analysis was done using proven tools like NPV, LCOE, PBP, IRR and ROI, previously used by other researchers (Riayatsyah et al., 2022), (Rönkkö et al., 2023), (Cali et al., 2018), (Butt et al., 2022), (Khajah & Philbin, 2022). These would serve as the economic indicators for the simulated offshore wind farm (OWF) model.

## 2. Methodology

### 2.1. Mathematical Modelling For Wind Resource

Kinetic energy (K.E.) of wind is dependent on the moving mass (m) of air and its speed (v), as in Equation [1].

$$\text{K. E.} = \frac{1}{2}mv^2 \qquad [1]$$

The rate of flow of this energy for a given time period (dt) gives the power ($P_W$) available in the wind as in Equation [2].

$$P_w = \frac{d(K.E.)}{dt} = \frac{1}{2}\frac{dm}{dt}v^2 \ \ Watts \qquad [2]$$

The mass flow rate ($\frac{dm}{dt}$) is the product of air density (ρ) and volume flow rate of the wind (Av) as given by Equation [3].

$$\frac{dm}{dt} = \rho \text{Av} \qquad [3]$$

Where: ρ = density of air, A = wind path swept area equivalent to area of turbine's blade swept by the moving mass of air.

 ISSN: 2957- 7780

And substituting Equation [3] into Equation [2], the Wind Power becomes as shown in Equation [4].

$$P_w = \frac{1}{2}\rho A v^3 \qquad [4]$$

From equation (4), the parameter ρ is a constant representing air density while A, is the swept area by the turbine's blade, and is specific for a particular wind turbine. The only variable parameter is the wind speed. It varies with time, location and altitude. The variation of place and time are already taken into consideration by the Lamu wind speed data collected by the Kenya Met.

The work presented in this paper, considered the wind speed data modeled to an altitude in accordance with a standard hub height of 50 m, mostly recommended by the simulation software. From the literature survey conducted, a standard calibration method called One-Seventh Power Law Method is used with referenced wind speed collected at a height of 10 m, the height at which the wind speed was collected by the Kenya Met.

The Power Law that governs the wind speed variation with altitude is given by [5].

$$\frac{v_1}{v_2} = \left(\frac{h_1}{h_2}\right)^{\alpha} \qquad [5]$$

From the literature survey conducted, the suitable value of $\alpha$ for most places is given by Equation [6].

$$\alpha = \frac{1}{7} = 0.14 \qquad [6]$$

Substituting Equation [6] into Equation [5], we get the Power Law relation as in Equation [7].

$$\frac{v_{10}}{v_h} = \left(\frac{h_{10}}{h_2}\right)^{\frac{1}{7}} \qquad [7]$$

Where:

- $v_{10}$= wind speed at a height of 10 m above the level surface
- $v_h$ = wind speed at the proposed turbine hub height in meters above the level surface
- $h_{10}$ = height of at which the Met. Wind data was collected = 10 m
- $h_2$ = the hub height of the proposed wind turbine.

For most simulation software tools, a wind turbine of hub height of 50 m is common and therefore the wind speed adjusted at a height of 50 m were considered and used in the HOMER software. Hence, for a wind turbine with a hub height of 50 m, the wind speed at this height is determined using the relation in Equation [8].

$$\frac{v_{10}}{v_{50}} = \left(\frac{10}{50}\right)^{\frac{1}{7}} \qquad [8]$$


ISSN: 2957- 7780

Hence wind speed at the 50 m is achieved as shown by Equation [9].

$$v_{50} = \frac{v_{10}}{(0.2)^{\frac{1}{7}}} \qquad [9]$$

Equation [9] can is simplified into Equation [10] shown.

$$v_{50} = \frac{v_{10}}{0.7946} \qquad [10]$$

For this work, equation (10) was considered and used to determine wind speed values that were modeled in the software.

### 2.2. Mathematical Modelling for Vision 2030 Projection of 50 MW Load Parameters.

#### 2.2.1 Mathematical Determination Of Number Of Wind Turbines Required.

The common turbines that find wide applications in the wind energy generations are Vestas and Siemens' types. Most suitable wind turbine that is increasingly used with current wind turbine technology is Vestas type. Available Vestas type wind turbine for Simulations are Vestas V47 (6,600 kW) with a hub height of 50 m; and Vestas (1.65 MW) with hub height of 70 m.

Now, number of wind turbines for a particular load demand is determined using equation (16).

$$\text{No. of wind turbines required} = \frac{Peak\ Load\ Demand\ in\ kW}{Wind\ turbine\ capacity\ in\ kW} \qquad [12]$$

Considering daily peak load demand of 50 MW and Vestas type wind turbine with hub height of 50 m, we have:

$$\text{No. of wind turbines required} = \frac{50{,}000\ kW}{660\ kW} = 76$$

#### 2.2.2 Mathematical Determination of Number of batteries required to provide an autonomy of 3 days.

Energy Requirement for autonomy (when wind speed is below cutoff speed or above cutout speed) say 3 days is:

Total Energy = Load × Duration
= 50 MW×72 hours
= 3,600 MWh

Accounting for energy losses during conversion, charging/discharging cycles, and environmental factors is key. Therefore, a typical efficiency of 90% wind was assumed for well-designed energy storage systems. Adjusted energy needed due to losses was thus determined using equation (13):

 ISSN: 2957- 7780

$$\text{Adjusted Energy} = \frac{\boldsymbol{Total\ Energy}}{\boldsymbol{Efficiency}} \quad [13]$$

$$= \frac{\boldsymbol{3600\ MWh}}{\boldsymbol{0.9}}$$

$$= 4000\ \text{MWh}$$

From the HOMER simulation software, battery with a maximum storage capacity of 1 MWh and a voltage range of 500V-800V is considered for use.

Number of batteries required was determined using equation (14).

$$\text{Number of Batteries} = \frac{\boldsymbol{Adjusted\ energy}}{\boldsymbol{Battery\ Capacity}} \quad [14]$$

$$= \frac{4000\ MWh}{1MWh}$$

$$= \boldsymbol{4000\ Batteries}$$

### 2.2.3 Mathematical Determination Of Number Of Converters Required.

Single phase converters, each rated at 240V were considered to supply battery storage system.

Output current of each converter was determined using equation (15).

$$\text{Output Current} = \frac{\boldsymbol{power}}{\boldsymbol{voltage}} \quad [15]$$

$$= \frac{\boldsymbol{50{,}000KW}}{\boldsymbol{240V}} = 208.33A$$

Based on this current rating, ABB PSTORE-PC converter rated at 2880kW at efficiency of 96% was considered.

From the typical converter efficiency, the actual output power was determined using equation (16):

$$\text{Actual power output} = \text{power rating x efficiency} \quad [16]$$

$$= 2880 \times 0.96$$

$$= 2764.8\ \text{kW}$$

Number of converters required was determined using equation (17):

$$\text{No. of converters} = \frac{\text{Average peak daily power in kW}}{\text{Actual converter output power in kW}} \quad [17]$$

$$= \frac{50{,}000KW}{2764.8\ \text{kW}}$$

$$= 18.06 \approx \boldsymbol{19}$$

## 2.3. Mathematical Modelling For Vision 2050 Projection of 200 MW Load Parameters.

### 2.3.1 Mathematical Determination of Number of Wind Turbines Required.

Number of wind turbines is determined using equation (16).


ISSN: 2957- 7780

Considering daily peak load demand of 50 MW and Vestas type wind turbine, V47 (6,600 kW), with hub height of 50 m, we have:

$$\text{No. of wind turbines required } = \frac{200{,}000\ kW}{660\ kW} = 304$$

**2.3.2 Mathematical Determination of Number of batteries required to provide an autonomy of 3 days.**

Battery, generic Li-Ion, with a capacity of 1 MWh and a voltage range of 500V-800V is chosen for use. Energy Requirement for autonomy, say 3 days is:

Total Energy = Load × Duration
= 2000 MW×72 hours
= 14,400 MWh

Considering losses as previously mentioned and taking efficiency typical efficiency of 90% for well-designed storage system, the adjusted energy needed due to losses was thus determined using equation (17). i.e.

$$\text{Adjusted energy} = \frac{\mathbf{14400\ MWh}}{\mathbf{0.9}}$$
= 16,000 MWh

From the HOMER simulation software, battery with a maximum storage capacity of 1 MWh and a voltage range of 500V-800V is considered for use. The number of batteries required was determined using equation (18). i.e.

Number of Batteries Required:

$$= \frac{\mathbf{16000MWh}}{\mathbf{1MWh}} = \mathbf{16000}\ \boldsymbol{Batteries}$$

**2.3.3 Mathematical Determination of Number of Converters Required.**

Single phase converters, each rated at 240V were considered to supply battery storage system and the output current of each converter was determined using equation (19). i.e.

$$\text{Output current} = \frac{200{,}000KW}{240V} 833.33A$$

From the value of current realized, ABB PSTORE-PC converter rated at 2880kW at efficiency of 96% was considered from HOMER software.

Number of converters required was then determined using equation (21):

$$\text{No. of converters} = \frac{\mathbf{200{,}000KW}}{2764.8\ \text{kW}} = 72.337 \approx \mathbf{73}$$


ISSN: 2957- 7780

### 2.4.Software Simulation

#### 2.4.1 Simulation Software Tool Consideration

The selection of the appropriate software for this work was enhanced after conducting literature survey. Comparison of the following RE tools was made in terms of general attributes, capability and complexity: System Advisor Model (SAM), Cost of RE Spreadsheet Tool (CREST), Renewable Energy Technology screen (RETsceen), WindPro, Windographer, Helloscope, Hybrid Optimization of Multiple Energy Resources (HOMER), Renewable energy optimization (Reopt) and Gatecycle., Regional Energy Development System (ReEDS), EnergyPLAN and KomMod.

From the tools listed above, only HOMER and REopt were observed to be capable of achieving the optimization results as part of the objectives of the work presented on this paper. It was also observed that Reopt is mainly used as optimization tool suitable for system sizing (Jo, 2017). For techno-economic planning and designs, HOMER software tool would give more detailed results for RE systems (Bahramara et al., 2016). To realize more detailed results in line with the desired techno-economic objectives, HOMER simulation tool would be capable of providing optimization, simulation and sensitivity analysis (Kumar et al., 2016).

HOMER software models are annual based i.e. the simulation software performs the energy calculations for 8.760 hours (Ayodele & Ogunjuyigbe, 2014). Hence it was chosen as a suitable software tool for the work presented here, whose main aim is to provide a comprehensive financial model for the techno-economic feasibility of the offshore wind energy system.

#### 2.4.2 HOMER Simulation

The inputs parameters into the software included: site or location and its specific resource i.e. wind speeds, site load profile data i.e. average daily peak power demand, and system components such as wind turbines, battery storage and converters, together with their numbers as determined from the mathematical models above.

The simulation process was repeated using each annual data for Lamu i.e. 2016, 2018, 2019 and 2020 for the two peak daily power demand projections of 50 MW by the year 2030 and 200 MW by the year 2050. These power demand projections used for this work were as provided by the Kenya Power and Lighting Company Limited, without any modification of the power demand data as provided.

For each year, a virtual wind-farm model was created and its operation are made in consecutive time-steps of either 8,760 hours or 525,600 minutes using HOMER Pro software. Hence the models here are annual-based systems.

 ISSN: 2957- 7780

Figure 1 shows a Virtual Wind Farm (VWF) model for the work presented here, and was created using peak daily load projection of 50 MW and the average monthly wind data for the year 2020 as well as the required system component specifications.

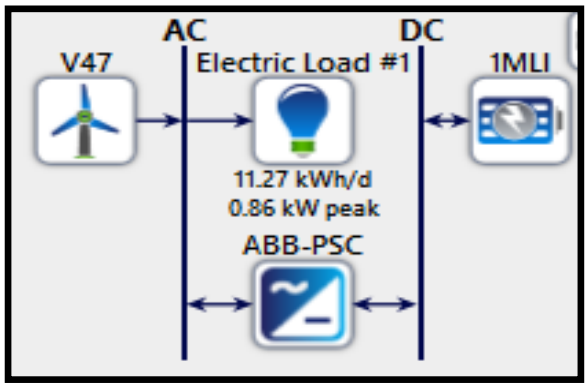


Figure 1: HOMER Simulation Model

Other Virtual Wind Farm (VWF) models similar to the one realized in figure 1 were also obtained in the repeated process using the data for the other years, already mentioned, 50 MW projection, and as well by using the 200 MW projection. For all the annual-based models used for the 50 MW and 200 MW as the average peak daily power demand projections for Lamu Port and its environs, the only variables involved in achieving different but similar models for each average daily power demand projection as above were the wind speeds.

## 3. Results and Discussion

During the simulation process, HOMER tool calculates the total cost of the VWF model over its projected life-time. Such costs include the Capital Expenditure (CAPEX), which is the total initial cost of the installing a wind-farm; Operation Expenditure (OPEX), which is the total cost for Operation and Maintenance (O&M) and the fuel cost; and replacement cost.

From the HOMER simulated VWF model for Lamu Port and its environs, two types of results were achieved: optimization results and sensitivity analysis results. The system optimization helps the user to plan the appropriate system sizing in order to meet the energy goals. Such goals include minimizing the costs of the system life-cycle and reduction of carbon emissions (Jo, 2017).

### 3.1. Optimization Results

HOMER Pro simulation tool used, runs several simulations in order to optimize the system. Optimal system implies the least Net Present Value (NPV) from the availed present values of all the costs over a life-time of the system. There are various criteria in which results can be sorted.


ISSN: 2957- 7780

The results presented in appendices A and B provided optimization results with several options of present values and from them there exists the one with the least present value for each OWF. HOMER Pro simulation to perform the sensitivity analysis to identify the most probable present value for each wind farm

### 3.2. Sensitivity Analysis

In the HOMER simulation for the offshore wind farm model, the software tool varied the available assumptions in order to realize the impacts of the results on the optimal system. The impacts were availed in tabulation, curves or graphical form. The sensitivity results were achieved for both the base case and the proposed system. With the future being uncertain, HOMER Pro simulation tool would be capable performing comparisons and providing the most possible outcomes presented as base case scenario analysis. For the sensitivity analysis result presented on this paper, HOMER Pro simulation tool considered base case results as the achieved outcomes with the most possible least costs. The sensitivity analysis results here include: daily, weekly or monthly power generation; monthly electricity production; cash flow by cost type and by component under nominal and discounted conditions and other economic indicator results such as NPV and LCOE.

Figures 2 and 3 show the daily power generation in MW achieved by using similar wind data the year 2020 wind speed data and the dynamic peak average daily power demand projections i.e. projections for the year 2030 projection of 50 MW as well as the projection for the year 2050 projection of 200 MW respectively.

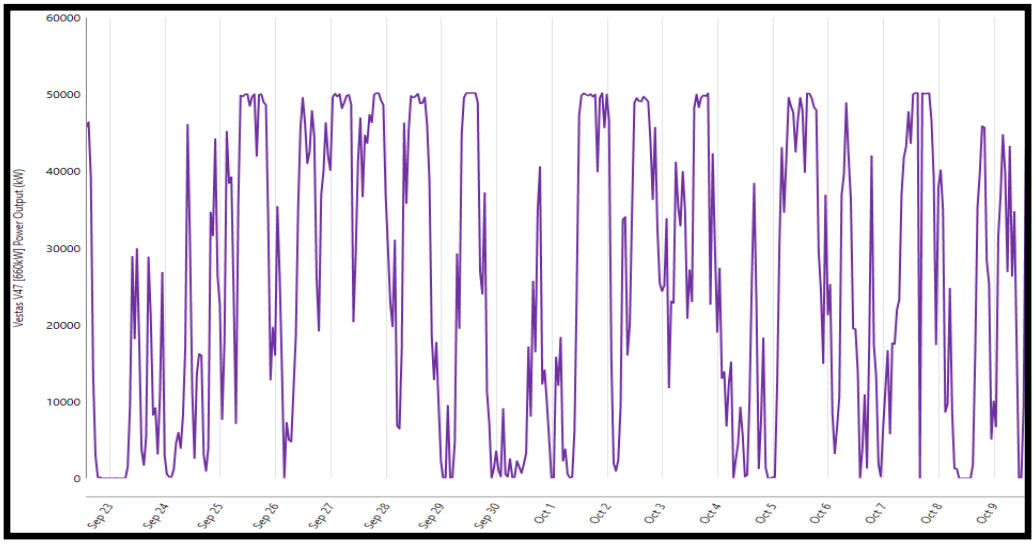


Figure 2: Daily Generation for Proposed Vision 2030 OWF


ISSN: 2957- 7780

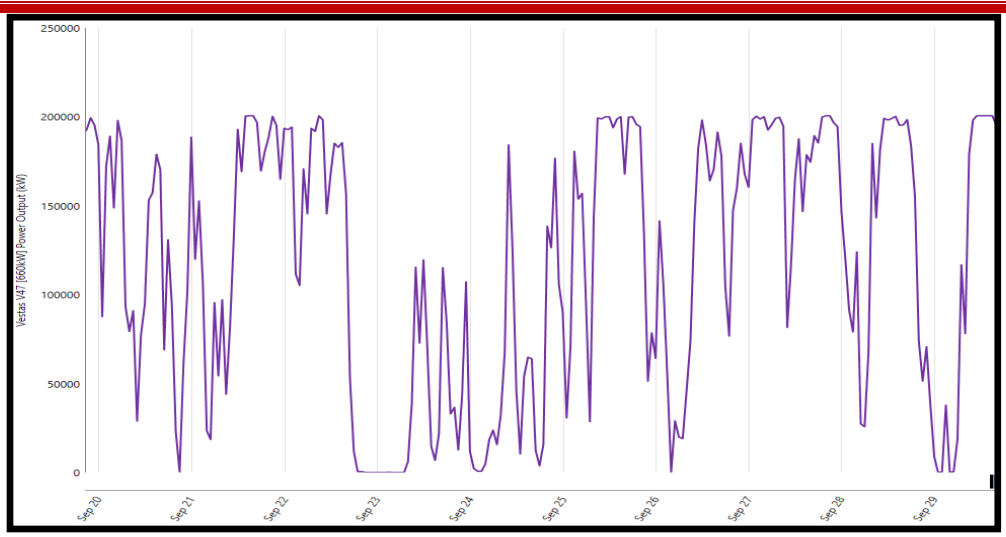


Figure 3: Daily Generation for Proposed Vision 2050 OWF

Figures 4 and 5 show the monthly average electrical energy to be utilized in MWh achieved by suing the 2020 wind speed data for and power demand projections for the years 2030 and 2050 respectively.

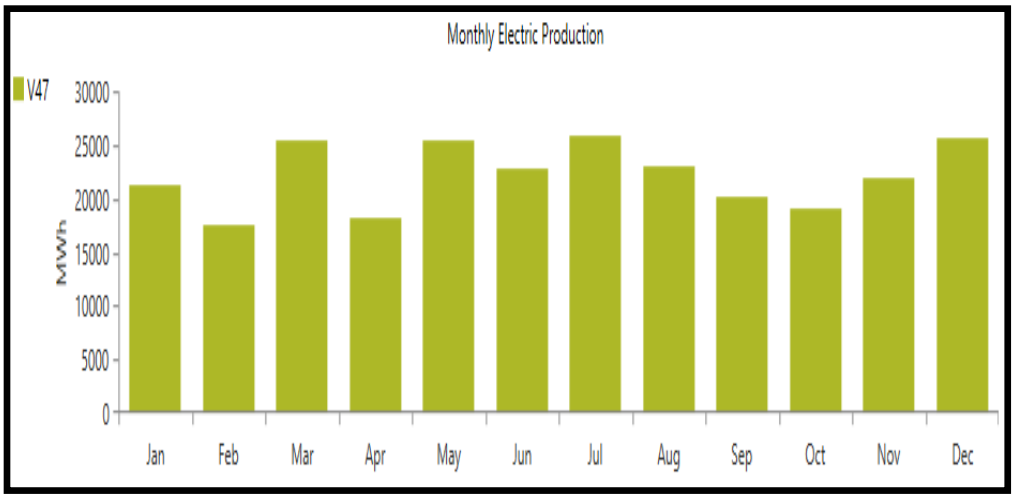


Figure 4: Monthly Electricity Production Proposed Vision 2030 OWF

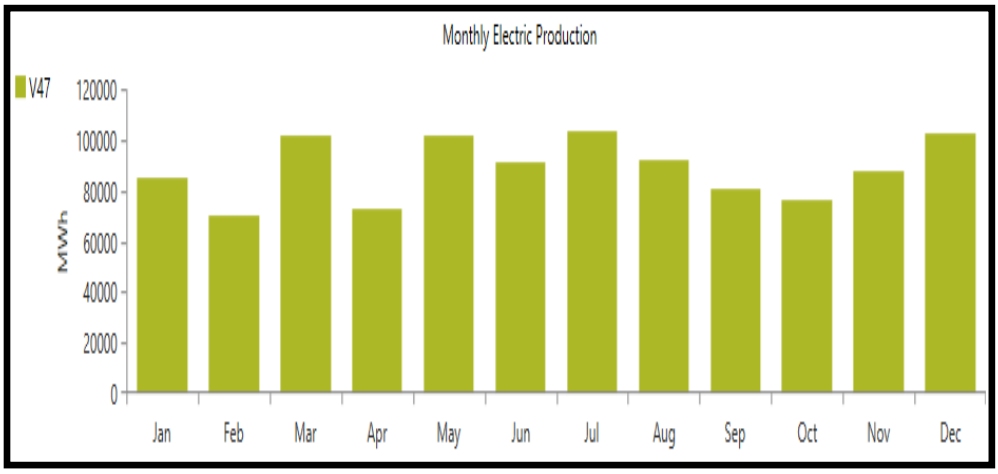


Figure 5: Monthly Electricity Production Proposed Vision 2050 OWF


ISSN: 2957- 7780

Figures 6 and 7 show the cash flow by cost type under nominal condition, achieved by suing the 2020 wind speed data for and power demand projections for the years 2030 and 2050 respectively. The nominal condition in this case refers to the acceptable working condition of the offshore wind farm that considers the cash inflow and outflow without any adjustment for future inflation.

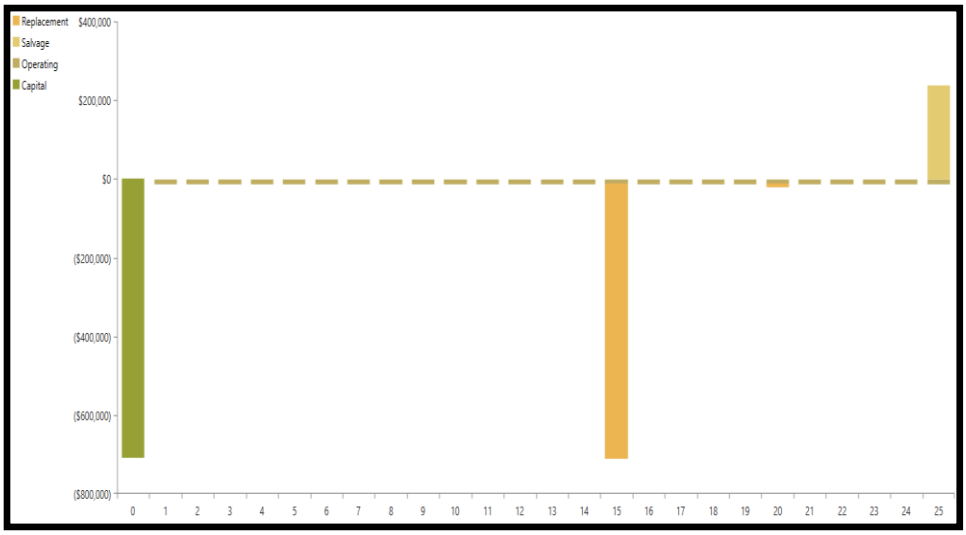


Figure 6: Cash Flow by Cost Type under Nominal Condition for Proposed Vision 2030 MW VWF

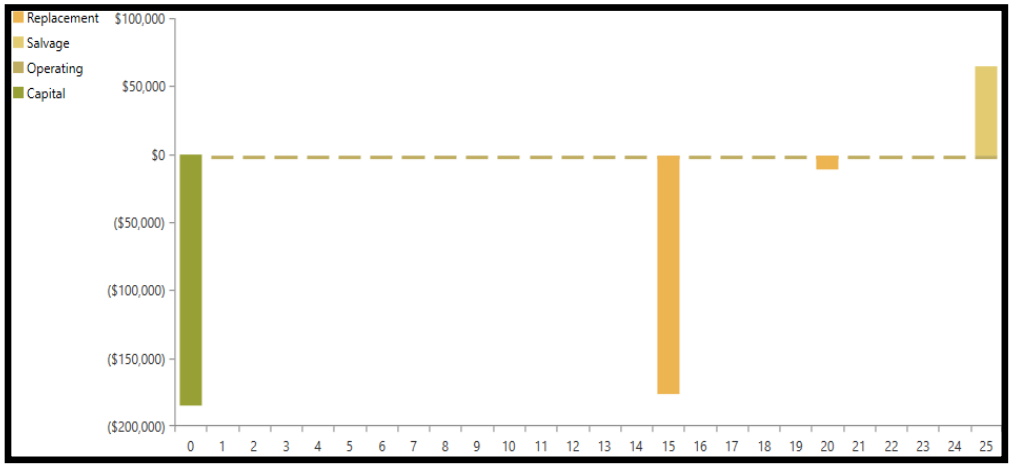


Figure 7: Cash Flow by Cost Type under Nominal Condition for Proposed Vision 2050 MW VWF

Figures 12 and 13 show the cash flow by cost type under discounted condition achieved by suing the 2020 wind speed data for and power demand projections for the years 2030 and 2050 respectively. Discounted condition refers to a condition of cash flow that incorporates the time value for money.


ISSN: 2957- 7780

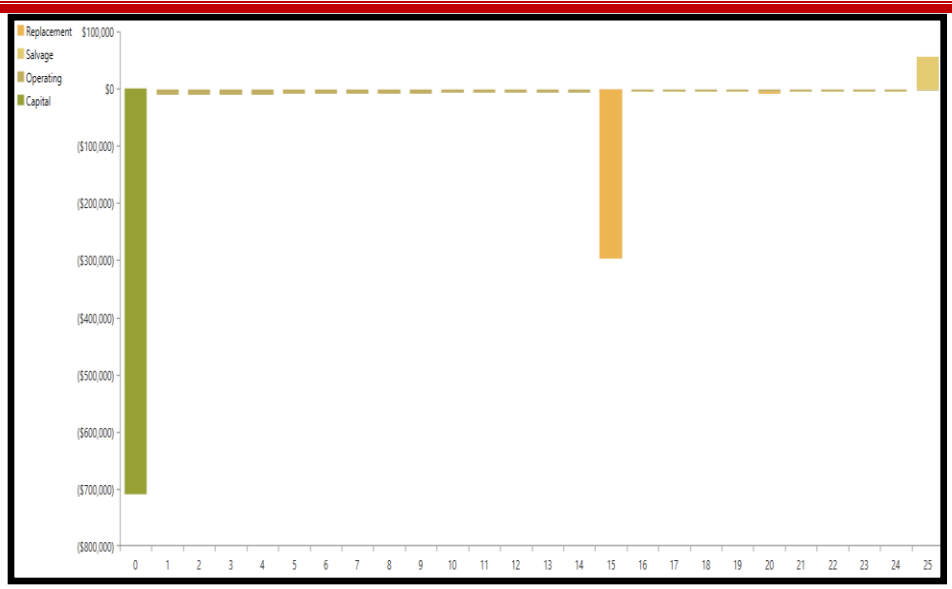


Figure 8: Cash Flow by Cost Type under Discounted Condition for Proposed Vision 2030 MW VW

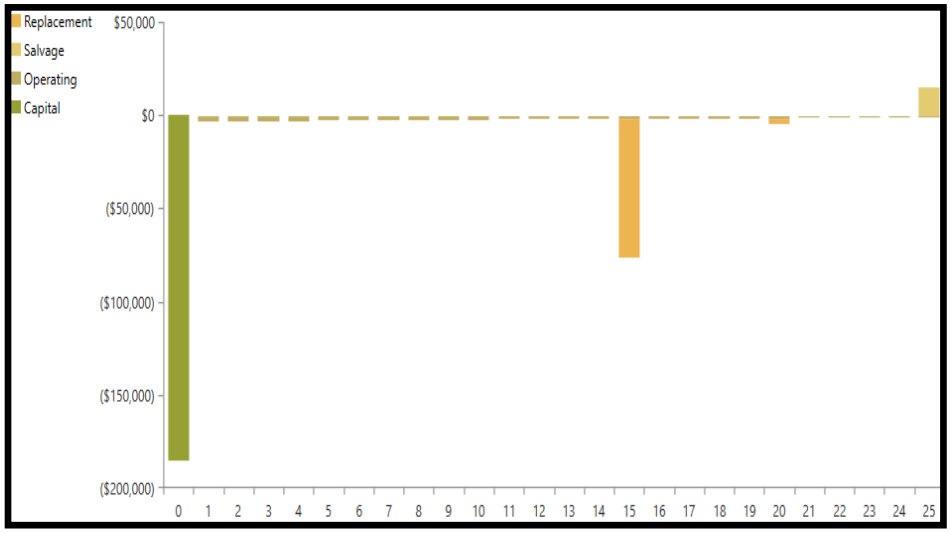


Figure 9: Cash Flow by Cost Type under Discounted Condition for Proposed Vision 2050 MW VWF


ISSN: 2957- 7780

### 3.2.1 Other Sensitivity Analysis Results

Table 3 shows some useful sensitivity results suitable decision making as per techno-economic aspect of offshore wind farm establishment in Lamu.

Table 3: Simulation Results for Energy Output, NPC, LCOE and Operating Cost

| | **Proposed 2030 Lamu OWF** | **Proposed 2050 Lamu OWF** |
|---|---|---|
| Annual Energy Output (kWh) | 266,204,237 | 1,064,816,947 |
| Total NPC ($) | 1,088,225.00 | 285,447.70 |
| Levelized COE ($/MWh) | 20.47 | 5.37 |
| Operating Cost ($) | 29,257.37 | 7,770,.07 |
| Payback Period (yr) | 3.36 | 3.19 |
| Internal Rate of Return (%) | 6.13 | 4.05 |
| Return on Investment (%) | 77.87 | 76.95 |

*From Study*

Alongside the graphical analysis results, other sensitivity results are presented in tabulation form. The tabulated results in this section were obtained using the same average monthly wind data for the year 2020, and the different projected load power for Lamu Port and its environs i.e. peak daily power demands of 50 MW by the year 2030 and 200 MW by the year 2050.

## 4. Conclusion

From figure 2 of average daily generation it was observed that the peak daily power produced by a projected 50 MW Lamu wind farm would be 50,160.00 kW. From figure 3, it was observed that the peak daily power produced by a projected 200 MW Lamu wind farm would be 200,640.00 kW (depicted by flat tips at the top of the curve). The capital cost and replacement cost for the proposed offshore wind farms for Lamu Port would be greatly reduced for 2050 offshore wind farm, both in proposed system and base case situations, as opposed to establishing the proposed 50 MW wind farm by 2030. In the fifteenth year of each plant's lifecycle, both of the proposed systems would have replacement cost being about but not equal to their respective capital cost. However, by the twentieth year of each plant's lifecycle, the replacement cost for both of the proposed plants, would be greatly reduced to $ 10,000. Hence replacement would not appropriate for pursuing before the twentieth year of the lifecycle period of each plant.

Under nominal condition, (figure 6), it was observed that the capital cost required to establish a 2030 projection of 50 MW Lamu offshore wind farm at year 0 would be $ 710,000.00, by the

15th year of the plant life, the replacement cost of the plant would be $ 700,000.00 while the replacement cost by the 20th year would be $ 10,000.00, and the salvage value by end of the plant life cycle would be $ 240, 833.33. From figure 7, still under the nominal condition, it was seen that the initial cost required to establish a 2050 projection of 200 MW Lamu offshore wind farm at year 0 would be $ 185,000.00, the replacement cost of the plant by the 15 year of the plant life would be $ 175,000.00, the replacement cost by the 20th year would be $ 10,000.00 while the salvage value by end of the plant life cycle would be $ 65, 833.33.

From figure 12, under discounted condition, it was observed that the capital cost required to establish the Vision 2030 projection of 50 MW Lamu offshore wind farm at year 0 would be $ 710,000.00, by the 15th year of the plant life, the replacement cost of the plant would be $ 296,991.68 while the replacement cost by the 20th year would be $ 3,188.07, and the salvage value by end of the plant life cycle would be $ 57, 693.52. Under discounted condition of figure 13, it was observed that the capital cost required to establish a 2050 projection of 200 MW Lamu offshore wind farm at year 0 would be $ 1850,000.00, the replacement cost of the plant by the 15th year of the plant life would be $ 74,247.92, the replacement cost by the 20th year would be $ 3,188.07 while the salvage value by end of the plant life cycle would be $ 15, 770.89.

For the operation expenditure cost, the simulation results revealed that the operating cost for the proposed Lamu OWF would be much decreased by 2050 as compared to proposed Lamu OWF by 2030. At the end of the plant's lifecycle, twenty-fifth year for each of the proposed systems, the salvage value for the 2030 Lamu OWF would be greatly higher than that of the proposed 2050 offshore OWF.

In terms of economic indicators, the proposed OWF would have a higher net present value by 2030 than that of the OWF by 2050. Nevertheless, the levelized cost of energy would be greatly produced for the 2050 system as compared to 2030 system. When evaluating the economic indicators, it would not be suitable to make an investment decision based on only one indicator with desirable result.

For the sake of NPV, a value greater than zero would be profitable, hence should be pursued. With the NPV equivalent to a value of zero, it would be an indication of neither gain nor loss and the project should not be pursued. Moreover, if the NPV would be of a value less than zero, it would be an indication of making loss and the project should not be pursued. Although the cost of establishing the proposed 2030 OWF seemed to be higher than that of the 2050 OWF in Lamu, the economic indicators from the simulation results depicted that the establishment of this wind

 ISSN: 2957- 7780

farm would still be economically viable. Since the NPV was positive i.e., the establishment of both 2030 OWF and 2050 OWF would be economically viable, hence suitable for pursuing.

The higher the percentage value of ROI, the greater the profitability that would be realized from an investment. Similarly, the IRR measures how fast the ROI would be realized, and the higher the value of IRR, the more the return on an investment would be realized. The simulated models showed that both proposed 2030 and 2050 offshore wind farms would have the ROI value above 70%, which would be a good indication of profitability from such investments. However, the IRR for the 2030 would be a bit higher than that of 2050 Lamu OWF.

The PBP would measure how long it would take to realize back the cost of an investment. An investment whose PBP would be realized after the end of a project's lifecycle should never be pursued. From the simulated model of 2030 and 2050 Lamu offshore wind farms, the PBP would fall between the third and fourth year, which would be a good indication that the investment costs would be realized early enough before the end of the proposed projects' life cycles. Hence both of the two proposed investments, would be suitable for pursuing.

**References**

Ayodele, T. R., & Ogunjuyigbe, A. S. O. (2014). *Mathematical methods and software tools for designing and economic analysis of hybrid energy system*. *9*(1).

Bahramara, S., Moghaddam, M. P., & Haghifam, M. R. (2016). *Optimal planning of hybrid renewable energy systems using HOMER : A review*. *62*, 609–611.

Butt, R. Z., Kazmi, S. A. A., Alghassab, M., Khan, Z. A., Altamimi, A., Imran, M., & Alruwaili, F. F. (2022). Techno-Economic and Environmental Impact Analysis of Large-Scale Wind Farms Integration in Weak Transmission Grid from Mid-Career Repowering Perspective. *Sustainability (Switzerland)*, *14*(5). https://doi.org/10.3390/su14052507

Cali, U., Erdogan, N., Kucuksari, S., & Argin, M. (2018). TECHNO-ECONOMIC analysis of high potential offshore wind farm locations in Turkey. *Energy Strategy Reviews*, *22*, 325–336. https://doi.org/10.1016/j.esr.2018.10.007

Derakhshan, S., Moghimi, M., & Motawej, H. (2018). *Development of a mathematical model to design an offshore wind and wave hybrid energy system*. *August*.

Jo, J. (2017). *A Comparative Analysis of Renewable Energy Simulation Tools: Performance Simulation Model vs. System Optimization Peter Tozzi Jr.[a], Jin Jo[a] , *.* 0–25.

Khajah, A. M. H. A., & Philbin, S. P. (2022). *clean technologies Techno-Economic Analysis and Modelling of the Feasibility of Wind Energy in Kuwait*. 14–34.

Kumar, P., Pukale, R., Kumabhar, N., & Patil, U. (2016). Optimal Design Configuration Using HOMER. *Procedia Technology*, *24*, 499–504. https://doi.org/10.1016/j.protcy.2016.05.085

*LAMU COUNTY INTEGRATED DEVELOPMENT PLAN September 2018 County Integrated*

 ISSN: 2957- 7780

*Development Plan ,*. (2022). *September 2018*.

LAPSSET Corridor Development Authority [LCDA]. (2016). *Brief on LAPSSET Corridor Project*. 47. https://vision2030.go.ke/publication/lapsset-project-report-july-2016/

Maandal, G. L. D., & Danao, L. A. M. (2021). *Techno-Economic Assessment of Offshore Wind Energy in the Philippines*.

Nyambegera, K. K. (2021). *The Maritime Commons : Digital Repository of the World Maritime A feasibility study of sustanaible offshore wind energy development in Kenya OFFSHORE WIND ENERGY DEVELOPMENT IN By in*.

REPUBLIC OF KENYA - Ministry of Energy. (2021). *Least Cost Power Development Plan*. *April*, 1–114.

Riayatsyah, T. M. I., Geumpana, T. A., Rizwanul Fattah, I. M., Rizal, S., & Indra Mahlia, T. M. (2022). Techno-Economic Analysis and Optimisation of Campus Grid-Connected Hybrid Renewable Energy System Using HOMER Grid. *Sustainability (Switzerland)*, *14*(13). https://doi.org/10.3390/su14137735

Rönkkö, J., Khosravi, A., & Syri, S. (2023). *Techno-Economic Assessment of a Hybrid Offshore Wind – Wave Farm : Case Study in Norway*.

Shu, Z. R., & Jesson, M. (2021). Estimation of Weibull parameters for wind energy analysis across the UK. *Journal of Renewable and Sustainable Energy*, *13*(2). https://doi.org/10.1063/5.0038001

 ISSN: 2957- 7780

# Enhancing Geothermal Drilling Efficiency: Kenyan Bentonite as a Versatile Drilling Mud

P. M. Weramwanja[1*], G. Rading[1], T. Ochuku[1], J. Kihiu[2], J. Borode[3]

[1]Mechanical and Manufacturing Engineering Department, College of Architecture and Engineering, University of Nairobi, Kenya

[2] Mechanical Engineering Department, Jomo Kenyatta University of Agriculture and Technology, Kenya

[3]Metallurgical and Minerals Engineering Department, Federal University of Technology Akure, Nigeria.

[*]Corresponding author: peter.weramwanja@mksu.ac.ke

***Article History***
*Submission Date: 21st August 2024*
*Acceptance Date: 15th September 2024*
*Publication Date: 30th September 2024*

## Abstract

Kenya's substantial geothermal potential, despite its significant contribution to the nation's energy mix, faces challenges due to high drilling costs, which account for nearly half of the total project expenditure. This study investigates the potential of locally sourced Kenyan bentonite as a cost-effective alternative for geothermal drilling fluids. Bentonite's unique properties, such as swelling, suspension capabilities, and colloidal dispersion, make it a promising candidate for enhancing drilling efficiency and reducing costs. Characterization of Kenyan bentonite, combined with polyvinyl alcohol (PVA), was conducted to assess its suitability for geothermal applications. Fourier Transform Infrared Spectroscopy (FTIR) revealed that the incorporation of PVA into the bentonite matrix results in reduced hydroxyl (O-H) stretching intensity, indicating effective hydrogen bonding and cross-linking. Zeta potential measurements demonstrated a significant increase in negative surface charge with higher bentonite content, suggesting enhanced electrostatic stability and improved dispersion of the composite materials. Thermal Gravimetric Analysis (TGA) showed that the PVA-bentonite composites exhibit superior thermal stability, with the PB20 sample achieving higher thermal degradation temperatures compared to pure PVA. The addition of bentonite also markedly enhanced the antioxidant activity of the composites, with PB20 demonstrating over 400% improvement in radical scavenging compared to neat PVA. These findings demonstrate the potential of Kenyan bentonite to enhance the performance of geothermal drilling fluids by improving thermal stability, surface charge properties, and antioxidant capabilities. The locally

sourced bentonite can serve as a viable alternative to imported drilling materials, stimulating economic growth in Kenya's geothermal sector. By reducing drilling costs, this resource can enhance the competitiveness and accessibility of geothermal energy. Furthermore, it provides a foundation for future research to expand its application in geothermal and other drilling domains.

**Keywords** - Kenyan Bentonite, Rheology, Drilling Mud, Polyvinyl Alcohol, Thermal Stability

## 1. Introduction

### 1.1. Overview of Bentonite in Geothermal Drilling Efficiency

Energy is a vital component of sustainable development, playing a critical role in the economic growth, development, and welfare of any nation (Dashti et al. (2021)). It is projected that global energy demand will increase by over 50% by 2040 (Rahman et al. (2022)). Despite the urgent need for alternative energy sources, fossil fuels remain the primary energy source worldwide due to their high energy density, contributing to over 30% of greenhouse gas (GHG) emissions (Maamoun et al. (2020)). Without a shift towards alternative sources, the increasing energy demand will inevitably lead to higher GHG emissions. Renewable energy sources are essential to mitigating these effects, playing a central role in combating climate change and achieving carbon neutrality (Osman et al. (2023)). Kenya, for example, possesses abundant renewable energy resources, with a natural energy mix predominantly consisting of geothermal, hydro, wind, and solar power, contributing approximately 70% of the nation's installed capacity (Takase et al. (2021)). Favorable geological conditions position Kenya as one of the lowest-cost developers of geothermal power globally, with an estimated potential of 10 GW (Merem et al., 2019). However, despite this potential, the current installed capacity is less than 1 GW, placing Kenya seventh worldwide in geothermal power production.

On the global scale, the number of geothermal exploration and drilling projects has significantly risen in recent decades (De Angelis et al. (2011); Sharmin et al. (2023) and Rolffs et al. (2017)). Geothermal energy is harnessed by drilling wells into geothermal reservoirs and transferring the Earth's heat via a circulating fluid, which is either extracted from the geothermal reservoirs or injected from the surface. (Finger et al. (2010)). One of the greatest challenges in the geothermal industry is the high cost of drilling operations, which constitutes about 50% of the total project cost, including both confirmation and development drilling. This significant expense directly contributes to the high cost of electricity for downstream consumers. Figure 1 illustrates the typical costs incurred in a 50 MW flash-steam geothermal

power generation plant, emphasizing the substantial portion attributed to drilling. (Bavadiya et al. (2019) and Randeberg et al. (2012)).

In drilling procedure, the cost of the fluid system is the single most important cost contributor, necessitating research and development to minimize the cost of fluids and ensure efficiency for maximum profits to be achieved. Despite the high cost, drilling fluid still has to be used Agwu et al. (2021).

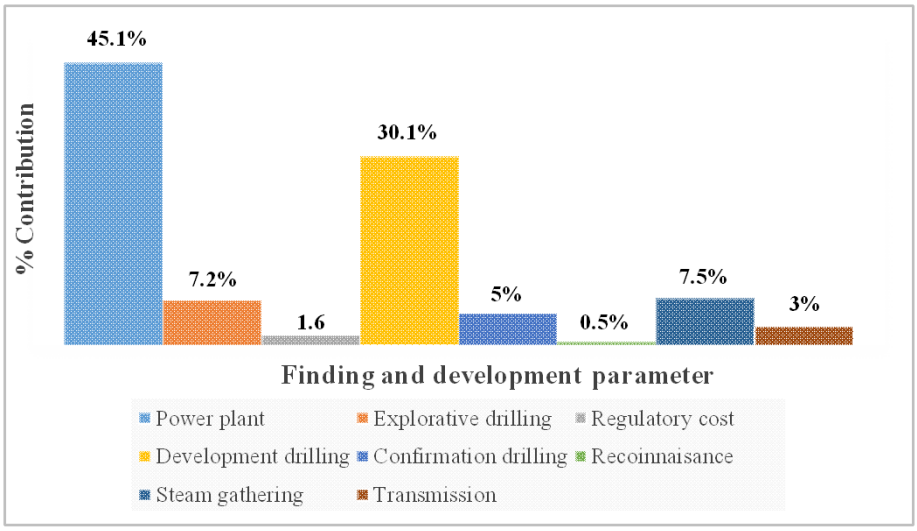


Figure 10: Exploration and development cost allocation for a typical 50 MW flash-steam geothermal power plant (Adapted from Bavadiya et al. (2019))

The need to reduce drilling costs is crucial for lowering electricity costs. The use of locally sourced materials such as Kenyan bentonite for drilling mud, can lower drilling costs, enhance foreign exchange savings, and thus, making geothermal projects more economically feasible. Bentonite, a clay with unique properties, plays a vital role in efficient drilling operations. By addressing these high drilling costs, the development of geothermal energy - a clean and renewable resource - can be accelerated, providing substantial benefits to the Kenyan population. According to Nyang'au et al. (2017), reducing drilling costs can significantly lower electricity prices, thereby enhancing overall living standards.

### 1.2. Drilling mud in geothermal applications

Drilling mud, an essential component of the drilling process serves multiple critical functions (Nasser et al., 2013). As a cooling agent, lubricant, and buoyancy medium, it facilitates drilling operations while ensuring borehole stability and pressure control. Additionally, drilling mud effectively transports and suspends cuttings from the drilling process, preventing borehole collapse and enabling geological data collection.

In the context of geothermal exploration, drilling mud plays an indispensable role in cooling and lubricating the drill bit, removing rock debris, and maintaining borehole stability. Its ability to suspend cuttings, provide buoyancy for the drill string, and form a protective mud cake is crucial for efficient drilling. Furthermore, drilling mud contributes to bit life extension, facilitates drilling in deviated wells, and aids in pressure management (Mohamed et al. (2021); Wakhyudin et al. (2017); Erge et al. (2020)). These diverse functions necessitate a drilling fluid with enhanced performance and environmental sustainability.

### 1.3. Kenyan Bentonite

Bentonite, first identified in the Cretaceous Benton Shale of Wyoming by Wilber C. Knight in 1898, has a rich history of diverse applications. Its initial uses spanned medicine, lubrication, and construction, with indigenous populations also recognizing its value (Hosterman et al. (1992)). Historically, river deltas provided natural deposits of bentonite-rich molding sand essential for ancient metalworking. The subsequent expansion of commercial and industrial applications spurred global bentonite mining.

Kenya possesses bentonitic clay deposits in regions such as the Athi River Basin, Timau, Meru, Amboseli and Namanga, as documented by the Department of Mining Economy and Maritime Affairs. However, a dearth of comprehensive characterization has limited the utilization of these domestic resources, with industries predominantly relying on imported bentonite (Rask, 1991; Ikua et al. (2017); Saggerson, (1991)).

Kenyan bentonite holds significant potential for diverse industrial applications due to its unique properties, such as swelling, forming water suspensions, and dispersing into colloidal particles (Mutisya et al. (2022)). These characteristics make it highly effective as an adhesive, suspension agent, and plasticizer, depending on the clay-to-water ratio. Additionally, bentonite can interact with organic materials to create organoclays, which are crucial in formulating drilling fluids, enhancing viscosity and stability, thus improving drilling efficiency and reducing costs (Repacholi, 2012; De Paiva et al. (2008)). Integrating locally sourced Kenyan bentonite in geothermal drilling operations leverages these properties and supports economic feasibility by reducing reliance on imports.

### 1.4. Enhancing the efficiency of Bentonite

A recent study has focused on the rheological properties of drilling mud such as gel strength, yield point, plastic viscosity, and apparent viscosity, which are essential for successful drilling operations (Agwu et al. (2021)). These properties directly influence the performance of drilling

mud. For example, plastic viscosity reflects the shape, size, and distribution of solid particles, affecting fluid flow resistance. High plastic viscosity can increase pump power usage and reduce penetration rates. Despite extensive studies on rheological properties, other crucial properties of drilling mud that significantly affect its functionality are often overlooked. For instance, the optical properties of drilling mud, particularly bentonite, are crucial for maintaining optimal performance in geothermal and oil well drilling operations. These properties allow for real-time monitoring and adjustment of the drilling fluid composition, which is essential for maintaining wellbore integrity and preventing issues such as clogging. By measuring turbidity and reflectance, the concentration of cuttings and particulates can be assessed, while the detection of gases or contaminants enhances safety and operational efficiency. Additionally, the optical characteristics help determine the particle size and distribution, which are necessary for the preservation of rheological properties and drilling stability. They also provide insights into heat absorption, reflection, and pressure variations, the factors which are critical for managing high temperatures and preventing pressure-related problems. Integrating nanotechnology into drilling fluids further enhances these processes, leading to more efficient, cost-effective, and environmentally friendly practices (Mohamed et al. (2021)).

Another property that remains underexplored is the thermal stability of drilling mud. Thermal stability is important due to temperature variations during drilling (Borges et al. (2022)). The improvement of this property can lead to more efficient drilling processes. Also, stabilization effects are essential for forming a filter cake on the borehole walls, minimizing fluid loss, and maintaining wellbore integrity. Furthermore, the adhesive properties of drilling mud, which affect interaction with the wellbore wall and drilling tools, are also critical. pH levels significantly impact corrosion control and the reaction of the mud with formation constituents (Gamal et al. (2019)). High pH levels, typically achieved using caustic soda (NaOH) or, increasingly, caustic potash (KOH), are necessary for managing wellbore contaminants and improving wellbore stability.

In geothermal drilling, reverse circulation involves the flow of mud through the drill pipe nozzles and return through the annulus, carrying cuttings produced by the bit. Drilling mud composition includes a base liquid (freshwater for geothermal drilling), active solids used (clays or polymers that determine viscosity), and inert solids (to vary density without affecting viscosity) (Hernandez et al. (2010)). Historically, a mixture of bentonite clay, freshwater, and polymer additives has been used to enhance drilling mud functionality and efficiency.

However, a significant challenge in geothermal drilling is lost circulation, which can account for up to 20% of well costs. This issue arises when drilling fluid is lost to fractures or pores in the rock formations (Carson et al. (1982)). One remedy involves using fibrous materials or particles in the drilling mud to plug these loss apertures. Understanding and improving the often-overlooked properties of drilling mud can help address lost circulation and reduce associated costs (Finger et al. (2012)).

By exploring additional properties and integrating advanced technologies, we can significantly enhance the efficiency and effectiveness of geothermal drilling processes, leading to improved operational performance and economic outcomes. Polyvinyl alcohol (PVA), known for its excellent film-forming and adhesive properties, was combined with bentonite, a natural clay with high adsorption capacity, to create composite films with enhanced mechanical and thermal stability. The suspensions of PVA and bentonite were prepared using a hot plate, mechanical mixer, and sonicator, while centrifugation ensured proper phase separation. Characterization of the films involved Fourier Transform Infrared Spectroscopy (FTIR), thermogravimetric analysis (TGA), and zeta potential measurements. These composite films, with tailored properties, hold potential for various industrial applications, particularly in fields requiring high-performance materials.

## 2. Materials and methods

### 2.1. Materials and Preparation of PVA and bentonite suspensions

Polyvinyl alcohol (PVA, 99% hydrolyzed) was acquired from Sigma-Aldrich Co. (St. Louis, Missouri, USA). The bentonite was locally obtained from three points in Isinya. 8 wt% of PVA suspension was prepared under constant agitation and heating at 100°C for 1hr on a hot plate. The PVA suspension was cooled to room temperature before further use. Similarly, 15 wt% Isinya bentonite suspension was prepared under constant stirring using a mechanical mixer for 30 mins. The bentonite suspension was homogenized for 10 mins by a sonicator (HD 2200, Bandelin Electronic Co., Berlin, Germany) at 72% power. Finally, the bentonite suspension was centrifuged at 10,000 RPM for 40 mins. The supernatant was mixed with the mid-layer and homogenized after which the solid content was adjusted to 8 wt% using deionized water to obtain the dissolved fraction and mid-layer. The PVA (P) and bentonite (B) suspensions were mixed in various proportions (PB0, PB10, PB15 and PB20) to form the casting solutions, where the number indicates the solid content of bentonite in the PVA matrix. The suspensions were solution cast to form the films for characterization.

### 2.2. Characterization

The chemical architecture of the neat bentonite, PVA and the composite films were analyzed by Fourier Transform Infrared Spectroscopy (FTIR) in attenuated total reflection (ATR) mode (FTIR, Excalibur FTS 3000, Bio-Rad, Hercules). The Zeta potential of the dispersions was assessed using the phase analysis light scattering (PALS) technique on a dynamic light scattering system (DLS, NanoBrook Omni). The thermal characteristics of the samples were investigated using a thermogravimetric analyzer ((TG209F3 Tarsus®) in a normal air atmosphere at a ramping rate of 10 °C/min.ABTS+ free radical scavenging assay technique was utilized to evaluate the antioxidant characteristics of the samples. The preparation and processing of the ABTS assay solution were done according to a previous report by Agumba et al. (2024). The antioxidant activity of the samples was assessed at 734 nm using Equation 1. The equation is not indicated.

$$\text{Antioxidant activity } (\%) = \left(\frac{A_c - A_s}{A_c}\right) 100 \qquad \text{Equation 1}$$

where $A_c$ indicates the absorbance of the control (ABTS) while $A_s$ is the sample absorbance.

## 3. Results and Discussion

Figure 2(a) depicts the FTIR spectra of bentonite, polyvinyl alcohol (PVA) and their composites (PB5-PB20), where the number represents the bentonite content in terms of weight percent (wt%). The characteristic bands of bentonite were found around 3426 cm–1 which correspond to O–H stretching and a deformation peak of H–O–H was observed at 1642 cm–1. Sharp bands due to Si–O stretching vibrations were found at 1035, 522 and 466 cm–1. For the PVA, the band around 3500 cm-1 were attributed to the O-H stretching vibrations while the bands around 1098 cm-1 and 1734 cm-1 correspond to C–O stretching and C=O groups respectively. The C=O groups in the PVA are linked to the presence of acetate groups. The band at 1000 cm-1 is due to -CH stretching vibrations of alkyl groups in the PVA. Upon loading different proportions of bentonite into PVA, additional bands were observed in comparison to PVA and bentonite. With increased loading of bentonite in the PVA matrix, the intensity of the O-H stretching bands around 3400-3300 cm-1 decreased. This decrease is ascribed to the active participation of the hydroxyl groups in the hydrogen bond-mediated chemical interaction between PVA and bentonite. The additional peaks at 1901, 1716, 1440, 1402, 1388 and 1255 cm–1 were ascribed to the chemical interactions between PVA and bentonite. The deformation and narrowing of H–O–H at 1601 cm–1 upon increasing bentonite content into

the PVA matrix signifies the crosslinking of the PVA network by bentonite and this may lead to a decrease in water absorption.

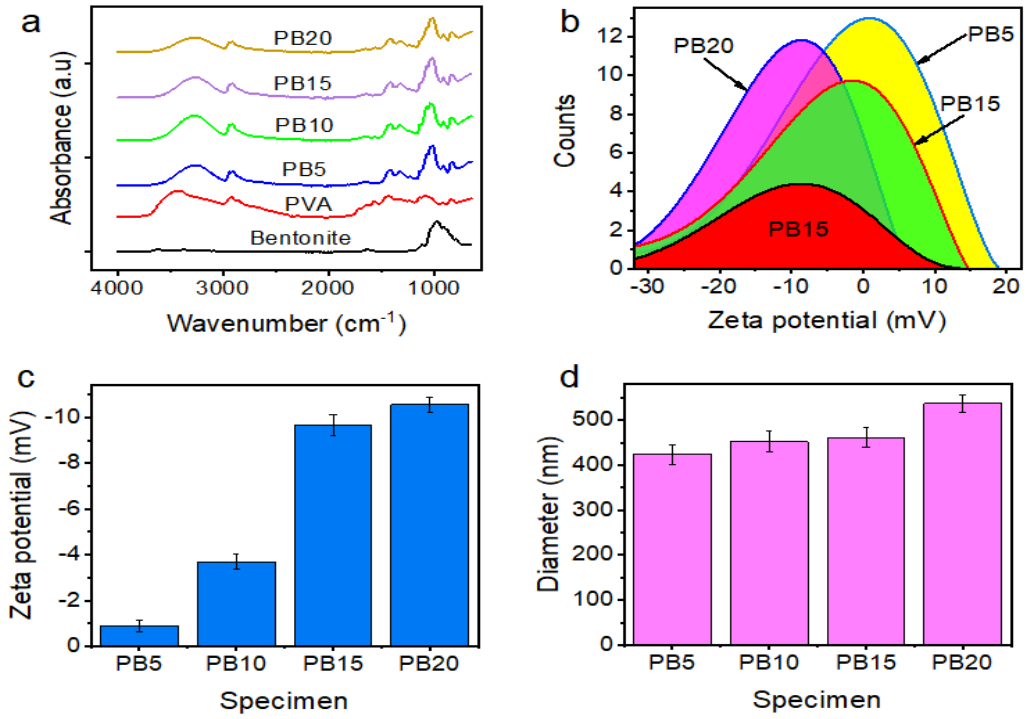


Figure 11: (a) FTIR spectra of bentonite, PVA, and their composites (PB5-PB20), (b-c) results of the surface charge properties of PVA/Bentonite composites and (d) effects of bentonite on the uniformity and dispersion stability

Zeta potential measurements were used to examine the surface charge properties of PVA/Bentonite composites as illustrated in Figure 2(b-c). The zeta potential of the composites significantly increased with the addition of the bentonite clay into the PVA matrix. All samples displayed a negative zeta potential value and did not exhibit any isoelectric point. This suggests that the electrokinetic potential is primarily controlled by the permanent layer charge in the bentonite. In terms of quantity, the changes in zeta potential values were more noticeable at higher bentonite loading with the PB20 revealing more electronegativity than PB5. These changes in the surface charge may indicate the involvement of electrostatic interactions or Van der Waals forces in the creation of the composite material. In the instance of asymmetrical molecules containing polar groups, such as PVA in its non-ionized state, electronic densities are found on the more electronegative components, resulting in dipoles that can interact with the negative charge of bentonite to create stable dispersions. Furthermore, from Figure 2(d), the presence of bentonite does not significantly increase the diameter of the molecules indicating the uniformity of the system and enhanced dispersion stability.

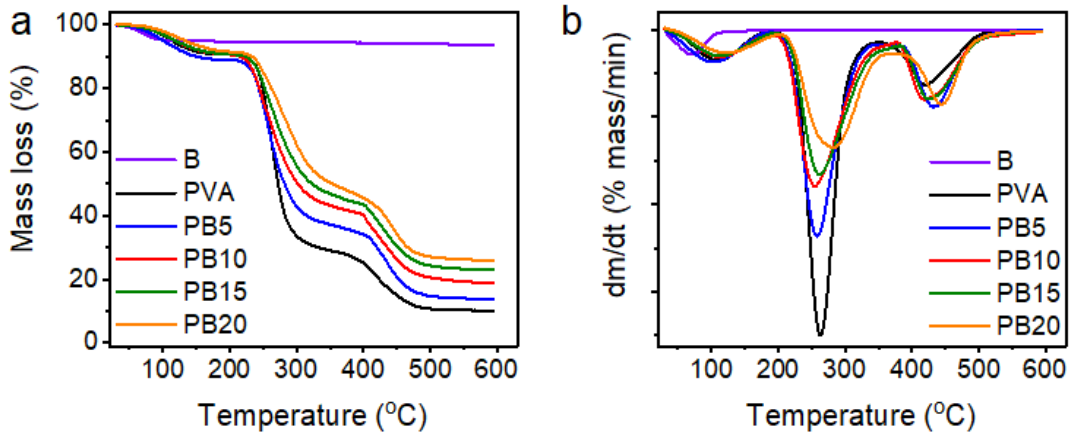


Figure 12: The experimental results of the neat PVA and bentonite clay along with their nanocomposites from the TGA and DTG analysis

Thermal characteristics were used to evaluate a material's thermal stability as well as its proportion of volatile elements by observing the decrease in weight of the specimen in a specific environment with changing temperatures. Figure 3(a-b) displays the experimental results of the neat PVA and bentonite clay along with their nanocomposites from the TGA and DTG analyses. In Figure 3(a), it can be observed that the mass loss of the samples reduces with increase in temperatures. The composites showed lower thermal degradation than the pure PVA sample since the bentonite clay shields the polymer from thermal degradation. All samples showed three clear degradation stages in the DTG results (Figure 3(b)). The initial weight loss occurred at approximately 70-128 °C as the moisture evaporated while heating. The primary weight loss happens between 200 to 300 °C for all samples, indicating the structural breakdown of PVA. The third phase is when the PVA's side chain breaks down at around 450°C. Maximum thermal stability is seen in PVA with 20 wt % bentonite clay, revealing a higher Td5%, Td10% and Tmax as indicated in Table 1, and this reveals nanoclay's impact on membrane thermal stability. The presence of nanoclay layers caused an enhancement in thermal stability by reducing the permeability of volatile degradation products and boosting heat insulation. Therefore, the thermal stability of the polymer composites significantly increased after bentonite was added to the PVA matrix.

Table 1: Thermal characteristics of the samples

| **Thermal Properties (°C)** | | | | | |
|---|---|---|---|---|---|
| **Specimen** | **Moisture loss** | | | | |
| PVA | 110.04 | 113.84 | 223.15 | 262.69 | 80.12 |
| PB5 | 103.73 | 101.16 | 150.20 | 257.27 | 93.98 |

| | | | | | |
|---|---|---|---|---|---|
| PB10 | 114.24 | 118.90 | 216.21 | 254.90 | 123.94 |
| PB15 | 114.30 | 119.30 | 224.36 | 261.02 | 112.96 |
| PB20 | 128.61 | 133.93 | 233.69 | 282.58 | 110.98 |
| Bentonite | 70.49 | 138.53 | | | |

Improving the antioxidant quality of substances is very important for eliminating free radicals. Therefore, the antioxidant characteristics of the composites were examined by conducting ABTS• assay to evaluate their capacity to eliminate ABTS•+ free radical cations as demonstrated in Figure 3(a-b). The PVA demonstrated an antioxidant function of about 4.5% proving to be ineffective in combating free radicals. By combining PVA with bentonite, enhanced antioxidant activity by over 400% was achieved for PB20 in comparison to the neat PVA. This finding shows that bentonite can function as a natural antioxidant, effectively suppressing free radicals to improve antioxidant qualities. Even though synthetic antioxidants are cost-effective, long-lasting and efficient, they pose risks as they are harmful, cancer-causing and not environmentally friendly. From this point of view, the method adopted in this study provides a straightforward, low-cost, eco-friendly, and sustainable approach to customize the antioxidant qualities of materials while maintaining their outstanding physical, thermal, and chemical attributes.

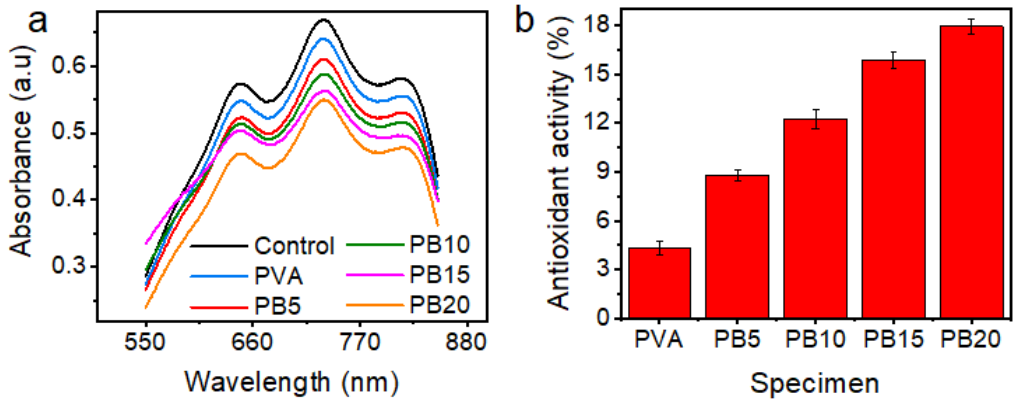


Figure 13: Examination of the antioxidant characteristics of the composites by conducting ABTS assay

## 4. Conclusion

In this study, investigations were carried out to determine the potential of Kenyan bentonite as a versatile drilling mud for the enhancement of geothermal drilling efficiency. Comprehensive characterization and formulation with polyvinyl alcohol (PVA) demonstrated that bentonite significantly enhances the thermal stability, surface charge properties, and antioxidant capabilities of the drilling mud. FTIR spectra showed that increasing bentonite content in the

PVA matrix results in reduced O-H stretching intensity, indicating effective hydrogen bonding and cross-linking. Zeta potential measurements revealed a marked increase in negative surface charge with higher bentonite loading, reflecting enhanced electrostatic stability and dispersion. Thermal analysis indicated that PVA-bentonite composites exhibit superior thermal stability, with PB20 showing higher thermal degradation temperatures compared to pure PVA. Additionally, the antioxidant activity of the composites improved dramatically, with PB20 achieving over 400% enhancement in radical scavenging compared to neat PVA. These improvements contribute to maintaining wellbore integrity and optimizing drilling operations. The integration of Kenyan bentonite in geothermal drilling offers a cost-effective, locally sourced alternative to conventional drilling fluids, reducing reliance on imported materials and supporting regional economic development. This research provides a solid foundation for future studies on scaling up the use of Kenyan bentonite in geothermal drilling and exploring its potential in other drilling technologies.

## Author contributions

**Peter Marko. Weramwanja:** Conceptualization, Methodology, Writing – Original Draft.

**John Muniu Kihiu:** Conceptualization, Supervision, Writing – review & editing**.**

**Joseph Olatunde Borode:** Conceptualization, Supervision, Writing – review & editing.

**George Odera Rading:** Resources,Investigation, Validation, Supervision, Editing.

**Thomas Ochuku Mbuya:** Resources, Editing.

## Conflict of interest

The authors declare that they have no known competing financial interests or personal relationships that could have appeared to influence the work reported in this paper.

## Acknowledgements

Science Initiative Group (SIG) supported this research through the African Materials Science and Engineering Network (AMSEN).

## References

Agumba, D. O., Kumar, B., & Kim, J. (2024). Advanced hydrostable, recyclable and degradable cellulose hybrid films as renewable alternatives to synthetic plastics. International Journal of Biological Macromolecules, 260, 129370.

Agwu, O. E., Akpabio, J. U., Ekpenyong, M. E., Inyang, U. G., Asuquo, D. E., Eyoh, I. J., &Adeoye, O. S. (2021). A critical review of drilling mud rheological models. Journal of petroleum science and engineering, 203, 108659.

Angelis-Dimakis, A., Biberacher, M., Dominguez, J., Fiorese, G., Gadocha, S., Gnansounou, E., ... &Robba, M. (2011). Methods and tools to evaluate the availability of renewable energy sources. Renewable and sustainable energy reviews, 15(2), 1182-1200.

Bavadiya, V., Srivastava, S., Salehi, S., &Teodoriu, C. (2019). Geothermal Drilling Training and Certification: Should it be Different. *In the 44th Workshop on Geothermal Reservoir Engineering. Stanford, California, USA.*

Borges, R. F. O., De Souza, R. S. V. A., Vargas, M. L. V., Scheid, C. M., Calçada, L. A., & Meleiro, L. A. C. (2022). Analysis of the stability of oil-based drilling muds by electrical stability measurements as a function of oil-water ratio, weighting material and lubricant concentrations. Journal of Petroleum Science and Engineering, 218, 110924.

Carson, C. C., & Lin, Y. T. (1982). Impact of common problems in geothermal drilling and completion (No. SAND-82-1374C; CONF-821007-10). Sandia National Labs., Albuquerque, NM (USA).

Dashti, A., &GholamiKorzani, M. (2021). Study of geothermal energy potential as a green source of energy with a look at energy consumption in Iran. Geothermal Energy, 9(1), 28.

De Paiva, L. B., Morales, A. R., &Díaz, F. R. V. (2008). Organoclays: properties, preparation and applications. Applied clay science, 42(1-2), 8-24.

Erge, O., Sakaoglu, K., Sonmez, A., Bagatir, G., Dogan, H. A., Ay, A., &Gucuyener, I. H. (2020). Overview and design principles of drilling fluids systems for geothermal Wells in Turkey. Geothermics, 88, 101897.

Finger, J. T., & Blankenship, D. A. (2012). Handbook of best practices for geothermal drilling (No. SAND2011-6478). Sandia National Lab.(SNL-NM), Albuquerque, NM (United States).

Gamal, H., Elkatatny, S., Basfar, S., & Al-Majed, A. (2019). Effect of pH on rheological and filtration properties of water-based drilling fluid based on bentonite. Sustainability, 11(23), 6714.

Hernandez, R., & Nguyen, H. (2010, April). Reverse-circulation cementing and foamed latex cement enable drilling in lost-circulation zones. In Proceedings World Geothermal Congress.

Hosterman, J. W., & Patterson, S. H. (1992). Bentonite and Fuller's earth resources of the United States (No. 1522).

Ikua, B. W., Maranga, S. M., & Mutisya, P. K. (2017). An Insight into the Sources of the Bentonite used in the Local Drilling Industry.

Maamoun, N., Kennedy, R., Jin, X., & Urpelainen, J. (2020). Identifying coal-fired power plants for early retirement. Renewable and Sustainable Energy Reviews, 126, 109833.

Merem, E. C., Twumasi, Y., Wesley, J., Olagbegi, D., Fageir, S., Crisler, M., ... & Washington, J. (2019). Analyzing geothermal energy use in the East African Region: The case of Kenya. Energy and Power, 9(1), 12-26.

Mohamed, A., Salehi, S., & Ahmed, R. (2021). Significance and complications of drilling fluid rheology in geothermal drilling: A review. Geothermics, 93, 102066.

Mutisya, P. K., Maranga, S. M., & Ikua, B. W. (2022, June). An Appraisal on the Potential uses of Bentonite and its Availability and Exploitation in Kenya. In Proceedings of the Sustainable Research and Innovation Conference (pp. 200-205).

Nasser, J., Jesil, A., Mohiuddin, T., Al Ruqeshi, M., Devi, G., &Mohataram, S. (2013). Experimental investigation of drilling fluid performance as nanoparticles. World Journal of Nano Science and Engineering, 2013.

Nyang'au, J., Nyakundi, P. A., Kemboi, E., & Makanga, J. T. (2017). Comparative Analysis in Physico-Chemical Properties of Locally Available Bentonite and Imported Wyoming Bentonite used in Geothermal Drilling in Kenya.

Osman, A. I., Chen, L., Yang, M., Msigwa, G., Farghali, M., Fawzy, S., ... & Yap, P. S. (2023). Cost, environmental impact, and resilience of renewable energy under a changing climate: a review. Environmental chemistry letters, 21(2), 741-764.

Rahman, A., Farrok, O., & Haque, M. M. (2022). Environmental impact of renewable energy source based electrical power plants: Solar, wind, hydroelectric, biomass, geothermal, tidal, ocean, and osmotic. Renewable and Sustainable Energy Reviews, 161, 112279

Randeberg, E., Ford, E., Nygaard, G., Eriksson, M., Gressgård, L., & Hansen, K. (2012). Potentials for cost reduction for geothermal well construction in view of various drilling technologies and automation opportunities. *In Proceedings, Thirty-Sixth Workshop on Geothermal Reservoir Engineering.*

Rask, M. (1991). Assessment of Parminter's bentonic clay in Meru District, Kenya.

Repacholi, M. H. (Ed.). (2012). Clay mineralogy: spectroscopic and chemical determinative methods. Springer Science & Business Media.

Rolffs, P., Richardson, J., & Amin, A. L. (2017). Innovative risk finance solutions: Insights for geothermal power development in Kenya and Ethiopia. Climate and Development Knowledge Network.

Saggerson, E. P. (1991). Ministry of Environment and Natural Resources, Mines and Geological Department, Kenya (No. 98). Report.

Sharmin, T., Khan, N. R., Akram, M. S., & Ehsan, M. M. (2023). A state-of-the-art review on geothermal energy extraction, utilization, and improvement strategies: conventional, hybridized, and enhanced geothermal systems. International Journal of Thermofluids, 18, 100323.

Takase, M., Kipkoech, R., & Essandoh, P. K. (2021). A comprehensive review of energy scenario and sustainable energy in Kenya. Fuel Communications, 7, 100015.

Wakhyudin, A., Setiawan, D., & Marjuan, O. D. (2017, December). Aerated drilling cutting transport analysis in geothermal well. *In IOP Conference Series: Earth and Environmental Science (Vol. 103, No. 1, p. 012008). IOP Publishing.*

# A Unified Symbol Error Rate (SER) Expression for Equal Gain Combining (EGC) and Maximum Ratio Combining (MRC) over Correlated Nakagami-m Fading Channels

E. Omosa*, P. O. Akuon, and V. O. Kalecha

School of Engineering, University of Nairobi, Nairobi, Kenya

*Corresponding author: edwinomosa@gmail.com

***Article History***
*Submission Date: 26th August 2024*
*Acceptance Date: 18th September 2024*
*Publication Date: 30th September 2024*

## Abstract

In this study, we present a unified expression for the Symbol Error Rate (SER) performance of M-ary Quadrature Amplitude Modulation (M-QAM) signals transmitted through arbitrarily correlated Nakagami-m fading channels with L diversity branches in additive white Gaussian noise (AWGN). We comprehensively analyze two prominent combining techniques: Maximal-Ratio Combining (MRC) and Equal Gain Combining (EGC) under these conditions. By deriving this expression, we aim to provide insights into the impact of fading severity, diversity order, and correlation between branches on the SER performance. To validate our theoretical findings, we present Monte Carlo simulation results, depicted graphically to highlight the variations in SER across different scenarios.

## 1. Introduction

The telecommunication industry is witnessing exponential growth, largely driven by the increasing demand for mobile communication services. As a result, high transmission rates have become a critical requirement in band-limited mobile communication systems [1][2]. M-QAM is particularly advantageous in this context due to its high spectral efficiency, enabling enhanced transmission rates without the need for additional bandwidth. Consequently, M-QAM is poised to be a key modulation scheme for next-generation wireless communication systems [1]-[4]. Despite these, channel fading remains a significant challenge that adversely affects the reliability and performance of wireless communication systems. Consequently, understanding and mitigating the effects of channel fading is essential for the design and

optimization of robust wireless communication systems, particularly in environments where high reliability and quality of service are critical.

Channel fading is a well-documented phenomenon that significantly impacts the performance and reliability of communication systems. To accurately characterize and predict the effects of fading, various statistical models have been developed, including Rayleigh, Nakagami-m, and Rician fading distributions [5]-[8]. Among these, the Nakagami-m distribution stands out due to its versatility and precision in modeling a wide range of real-world propagation environments. It is particularly favored because it can accurately replicate experimental data across diverse scenarios, making it a valuable tool in wireless communication research.

The Nakagami-m distribution is also noteworthy for its ability to approximate other fading models, such as the Rician distribution, while inherently including Rayleigh fading as a special case. The Rician distribution, while theoretically important, presents analytical difficulties due to the presence of Bessel functions in its probability density function (PDF) [7][8]. These mathematical complexities often complicate the derivation of closed-form expressions, limiting its practical utility in some cases.

To counteract the detrimental effects of channel fading, receiver diversity techniques have been widely adopted in communication systems. These techniques are recognized for their cost-effectiveness, simplicity, and efficacy [6]. By exploiting the principle that multiple replicas of a signal are unlikely to undergo deep fading simultaneously, receiver diversity significantly enhances signal reliability. Among the most prominent spatial diversity techniques are MRC, SC, and EGC [9][10]. Each of these methods offers distinct advantages and trade-offs, making the choice of an appropriate scheme highly dependent on the specific requirements and constraints of the communication system.

MRC is widely recognized as the most effective diversity scheme, offering the best performance in terms of signal-to-noise ratio (SNR) improvement. This superior performance is achieved by weighting and coherently summing the received signals from all diversity branches in proportion to their SNR. However, the complexity of MRC is significant, as it requires the receiver to estimate the channel gain of each branch accurately and then combine these branches optimally [9][10]. This process demands substantial computational resources and precise synchronization, which may not be feasible in all practical applications.

On the other hand, SC represents the simplest and least complex diversity technique. SC receivers prioritize the branch that has the strongest signal at the time of reception and discard

the weaker ones. While this method significantly reduces the computational burden and simplifies implementation, it offers the lowest performance among the three techniques, as it does not fully exploit the diversity potential of the system [9][10].

EGC offers a compromise between MRC and SC. In EGC, the signals from all diversity branches are combined with equal weights, without requiring precise channel estimation. Although EGC does not achieve the optimal performance of MRC, it provides better performance than SC while maintaining a relatively moderate level of complexity [9][10]. This balance between performance and complexity makes EGC a viable option in scenarios where the computational resources are limited, but higher reliability is still desired.

Lastly, when the diversity branches are adequately separated, the assumption of independent fading for each branch is generally valid. However, in cases where the branches are closely spaced, the received signals may become arbitrarily correlated, making analysis and performance prediction more challenging [4]-[7]. Despite extensive research on the performance of M-QAM signals under various fading conditions, most studies have been limited to a single combining technique, either in uncorrelated or correlated channels [11]-[15]. A comprehensive expression that accounts for multiple combining techniques is elusive. Additionally, much of the research has focused on two-branch Single Input Multiple Output (SIMO) systems. While these studies offer valuable insights, there is an increasing need to extend the analysis to multi-branch systems to better understand and mitigate the effects of correlated fading in more complex communication scenarios. This paper addresses this gap by extending the analysis to multi-branch SIMO systems operating over Nakagami-*m* fading channels. Furthermore, we derive a simple yet accurate unified expression for MRC, and EGC in such correlated Nakagami-*m* fading environments, providing a valuable tool for performance evaluation.

**Motivation**

Existing SER expressions for correlated M-QAM signals in SIMO systems are often computationally complex. These expressions typically require channel estimation for the desired signal, and crucial system parameters, such as fading characteristics, are frequently obscured within hypergeometric functions. Moreover, many of the available SER expressions involve integral functions with exponential sums, making them difficult to analyze and apply.

Additionally, these expressions are often constrained to specific ranges of average SNR, which further complicates their application in practical scenarios. Given these challenges, there is a

clear need for a simplified, accurate, and closed-form expression for the SER in correlated Nakagami-m fading channels that unifies various diversity combining techniques and accounts for multi-branch receive systems across the entire range of SNR values. This paper aims to address these needs by deriving such an expression, which we believe will facilitate the design and evaluation of communication systems functioning in challenging environments.

**Organization**

This paper is structured as follows: Section 1 introduces the topic. Section 2 describes the system model. Section 3 examines system performance. Section 4 discusses the results. Section 5 concludes the paper.

**Notation**

This paper uses bold uppercase symbols to represent matrices and regular letters to represent scalar values. The Gaussian Q-function is denoted by Q(.). Moreover, E(.) is used for the expectation, $(.)^*$ for the complex conjugate, and $(.)^H$ for the Hermitian operator.

## 2. System Model

A SIMO diversity system with $L$ receive antennas is considered. Each channel is conceptualized as a Nakagami-m fading channel with AWGN. The AWGN is a zero-mean, $\mu = 0$, complex Gaussian random variable with a variance , $\sigma^2 = N_0$ /2, where $N_0$ denotes the single-sided power spectral density (PSD) of the noise.

The modulated MQAM signal transmitted over a Nakagami-m fading channel has a transfer function given by:

$$c(t) = \alpha . e^{j\theta} \tag{1}$$

The received signal at the $L_{\text{th}}$ branch over the symbol duration is expressed as:

$$r_L(t) = \alpha_L e^{j\theta_L} . s(t) + n_L(t) \tag{2}$$

where s(t) is the transmitted modulated signal, $n_L(t)$ represents the AWGN, $\theta_L$ is the phase of the channel, uniformly distributed over the interval $[0,2\pi]$ during a single signal interval, and $\alpha_L$ is the Nakagami-*m* fading envelope with a PDF as expressed in [7]-[8].

$$P_\alpha(\alpha) = 2\left(\frac{m}{\Omega}\right)^m \frac{\alpha^{2m-1}}{\Gamma(m)} exp\left(-\frac{m\alpha^2}{\Omega}\right) \tag{3}$$

where *m* is the fading severity parameter, varying from 0.5 to infinity, and $\Omega$ =E($\alpha^2$) is the average power. For *m* = 1, *m*=0 and *m*=∞, the Nakagami-*m* distribution corresponds to

Rayleigh, one-sided Gaussian, and non-fading channels, respectively [10]-[13]. The Gamma function Γ ($m$) is defined by:

$$\Gamma(m) \int_0^{\infty} y^{m-1} \exp(-y)\, dy \tag{4}$$

The received instantaneous SNR is defined as $\gamma = \alpha^2 \frac{E_s}{N_0}$, where $E_s$ is the symbol energy. The average SNR is given by $\bar{\gamma} = E[\gamma] = E\left[\alpha^2 \frac{E_s}{N_0}\right] = E[\alpha^2] \frac{E_s}{N_0}$. Assuming $E[\alpha^2] = \Omega = 1$, then $\bar{\gamma} = \frac{E_s}{N_0}$.

### 2.1. Diversity Decorrelation

Figure 1 presents the implementation of the decorrelation model within an $L$-branch receive diversity system. The correlated signals received from the $L$ branches are combined using an appropriate diversity combiner, such as MRC, or EGC, and subsequently equalized to obtain an estimate of the transmitted symbol $\acute{x}(0, c)$, where c denotes the type of combiner employed. When the estimated symbol traverses a channel characterized by a combined coefficient $\hat{h}(0, c)$, the resulting combined signal output is given by $\acute{r}(0,c) = \hat{h}(0, c)\acute{x}(0, c)$. For the purpose of analyzing the $L$ correlated signals, the combined signal output is routed through a power splitter, where a transformer decomposes it into L independent symbols $\acute{\hat{x}}_{(m,c)}$, with $m \in [1: L]$, as depicted in Figure 1. A suitable transformer for such an application is the Eigenvalue Decomposition (EVD) [2][8]-[12].

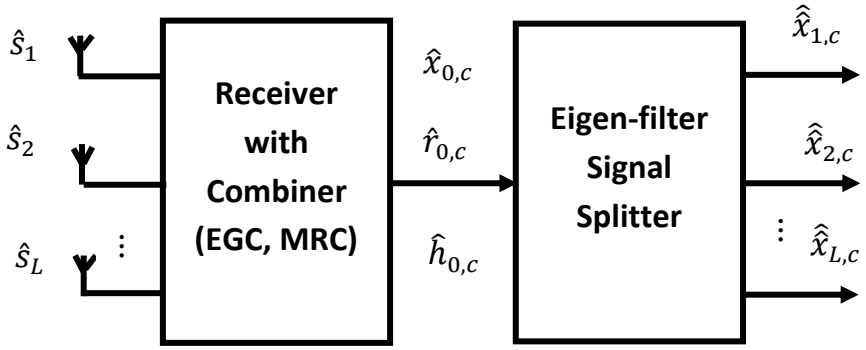


Figure 1: Diversity Decorrelation System

The spatial correlation between signals received from any two branches can be represented by the correlation coefficient $\rho_{kl}$ [15][16].

$$\rho_{kl} = \frac{E[\hat{h}_k \hat{h}^*{}_l]}{\sqrt{\sigma^2_{\hat{h}_k} \sigma^2_{\hat{h}_l}}}, l, k = 1,2, \dots N_r \quad (5)$$

where $\sigma^2_{\hat{h}_k}$ is the variance of the random variable (RV) $\hat{h}_k$ and $\sigma^2_{\hat{h}_l}$ is the variance of the RV $\hat{h}_l$

By defining $\boldsymbol{R}$ as the normalized correlation matrix, it can be formulated as [16][17]:

$$\boldsymbol{R} = \begin{pmatrix} 1 & \rho_{12} & \cdots & \rho_{1L} \\ \rho_{12} \vdots & 1 & \ddots & \rho_{2L} \vdots \\ \rho_L & \dots & \cdots & 1 \end{pmatrix} \quad (6)$$

The matrix $\boldsymbol{R}$ is assumed to be positive-definite with positive eigenvalues [17]. It can be decomposed into orthogonal eigenvectors and eigenvalues using the EVD process. This process can be expressed as follows [18][19]:

$$\Lambda = \boldsymbol{Q}\boldsymbol{R}\boldsymbol{Q}^H$$

$$\Lambda = \begin{pmatrix} \lambda_1 & 0 & \cdots & 0 \\ 0 & \lambda_2 & \cdots & 0 \\ \vdots & \vdots & \ddots & \vdots \\ 0 & 0 & \cdots & \lambda_L \end{pmatrix} \quad (7)$$

The eigenvalues are represented by $[\lambda_1, \lambda_2, \dots \lambda_L]$, while Q represents the matrix of eigenvectors. The matrix of positive eigenvalues is denoted by $\boldsymbol{\Lambda}$. The EVD process yields the matrix $\boldsymbol{Q}$, whose rows are orthonormal basis elements. This makes $\boldsymbol{Q}$ a unitary transformation. Additionally, $\boldsymbol{Q}^H$=$\boldsymbol{Q}^{-1}$.

### 2.2. Eigen-filter Operation

The theory of eigen-filter operation is comprehensively expounded in [17]. Here, the authors present the equivalent channel coefficient for the $k_{th}$ output branch as:

$$\hat{h}_k = \sqrt{\boldsymbol{\epsilon}_k}\widehat{\boldsymbol{Q}}_k \widehat{\boldsymbol{Q}}_k = \sqrt{\boldsymbol{\epsilon}_k}\widehat{\boldsymbol{Q}}_k \hat{\hat{\boldsymbol{h}}} \quad (8)$$

where: $\boldsymbol{\epsilon}_k \in \Lambda$ and $\widehat{\boldsymbol{Q}}_k$ is the $k_{th}$ column of $\widehat{\boldsymbol{Q}}$. $\hat{\hat{\boldsymbol{h}}}_k$ denotes the approximated Nakagami-m fading channel in a correlated system. The channel coefficients are complex numbers with a random amplitude and a uniformly distributed phase between 0 and 2π.

As noted in [20], the product of $\widehat{\boldsymbol{Q}}_k$ and $\hat{\hat{\boldsymbol{h}}}$, ($\hat{Q}_k \hat{\hat{\boldsymbol{h}}}$), has independent elements. Consequently, correlated paths can be analyzed as independent branches with scaled eigenvalues. Because the matrix $\boldsymbol{Q}$ is usually derived from $\boldsymbol{R}$ or given as input, $\boldsymbol{Q}$ is considered a blind estimate, and $\boldsymbol{R}$ does not require measurement.

## 3. Combiner average output SNR

### 3.1. Maximum Ratio Combining

The instantaneous SNR of the MRC-combined signal is provided in [4][6][9] as:

$$\gamma_{MRC} = \frac{\sum_{i=1}^{L} \propto_i^2 E_b}{N_0} = \sum_{i=1}^{L} \gamma_i \tag{9}$$

The mean output SNR for receiver diversity utilizing MRC can be determined by taking the expectation of the instantaneous output SNR for a specified number of receive antennas *L*, as evaluated in [6][21].

$$\overline{\gamma}_{0,MRC} = E|\gamma_{MRC}| = L\overline{\gamma}_{0,i,MRC} \tag{10}$$

where $\overline{\gamma}_{0,i,MRC}$ represents the optimal mean output SNR, and $\gamma_{MRC} = \sum_{i=1}^{L} \gamma_i = 1$.

### 3.2. Equal Gain Combining (EGC)

Assuming independent fading paths and utilizing *L* receive antennas, let the received symbol at each antenna i be denoted by $r_i$. Following processing by the EGC combiner, the symbol associated with the $i_{th}$ antenna is expressed as:

$$\acute{r}_i = \sum_{i=1}^{L} r_i \tag{11}$$

The signal delivered by the $i_{th}$ antenna path is given by signal $r_i = \propto_i \sqrt{E_s} + n_i$. This signal is influenced by the random fading amplitude $\propto_i$ of the $i_{th}$ symbol, the symbol energy $E_s$, and the AWGN component $n_i$ at the receiver. The AWGN component follows a zero-mean Gaussian distribution with variance $\sigma^2 = N_0/2$.

The combiner output results in the conditional SNR per symbol, denoted as $\gamma_{0,EGC}$, for symbols transmitted with equal power is given as:

$$\gamma_{0,EGC} = \frac{(\sum_{i=1}^{L} \propto_i)^2 E_s}{\sum_{i=1}^{L} N_i} \tag{12}$$

where $N_i$ represents the AWGN introduced into the signal, characterized by a power spectral density. Assuming independent paths and equal PSD, $N_0$, for the AWGN, the mean output SNR, denoted as $\overline{\gamma}_{0,EGC}$ for the EGC, can be expressed as the mathematical expectation of Equation (12).

$$\overline{\gamma}_{0,EGC} = \frac{E_s}{LN_0}\left[\sum_{i=1}^{L} E\{|\propto_i|^2\} + \sum_{i=1}^{L}\sum_{j\neq i}^{L}\sum_{j=1}^{L} E(\propto_i)E(\propto_j)\right] \quad (13)$$

At the ith and jth antennas, let the received symbols be denoted as $r_i = \propto_i \sqrt{E_s} + n_i$ and $r_j = \propto_j \sqrt{E_s} + n_j$, respectively. Removing the superscripts for simplicity, $E[\acute{r}^2]$ is expressed as:

$$E[\acute{r}^2] = \sum_{i=1}^{L}\sum_{j=1}^{L} E(r_i r_j)$$

$$= \sum_{i=1}^{L}\sum_{j=1}^{L} E\left(\propto_i \propto_j E_s + \propto_i \sqrt{E_s} n_j + \propto_j \sqrt{E_s} n_i + n_i n_j\right) \quad (14)$$

The objective is to devise a blind method that dispenses the necessity of transmitting known training symbols to estimate the SNR. Consequently, we propose an SNR estimator based on the received symbols. Positing a Nakagami-m distribution for $\propto$ and $[\propto^k] = \frac{\Gamma\left(m+\frac{k}{2}\right)}{m^{k/2}\Gamma(m)}$, it follows that $[\propto^2] = \Omega = 1$ and $E[\propto] = \frac{\Gamma\left(m+\frac{1}{2}\right)}{\sqrt{m}\Gamma(m)}$. It can be demonstrated that:

$$E[\acute{r}^2] = L\left[1 + (L-1)\frac{\Gamma^2\left(m+\frac{1}{2}\right)}{m\Gamma^2(m)}\right]E_s + L\sigma^2 \quad (15)$$

As the $\propto$ values are independent of the noise terms n, it follows that:

$$E[\acute{r}^2] = E_s \sum_{i=1}^{L}\sum_{j=1}^{L} E(\propto_i)E(\propto_j) = L\left[1 + (L-1)\frac{\Gamma^2\left(m+\frac{1}{2}\right)}{m\Gamma^2(m)}\right]E_s \quad (16)$$

$$\sum_{i=1}^{N_r}\sum_{j=1}^{N_r} E(\propto_i)E(\propto_j) = L\left[1 + (L-1)\frac{\Gamma^2\left(m+\frac{1}{2}\right)}{m\Gamma^2(m)}\right] \quad (17)$$

Assuming that the average SNR across the diversity branches is $\overline{\gamma}_i = \frac{\Omega_i E_s}{N_0} = \overline{\gamma}$, it can be shown that Equation (13) can be expressed as:

$$\overline{\gamma}_{EGC} = \left[1 + (L-1)\frac{\Gamma^2\left(m+\frac{1}{2}\right)}{m\Gamma^2(m)}\right]\overline{\gamma}$$

$$\approx L\left(1-\frac{1}{5m}\right)\overline{\gamma}$$

( 18 )

Equation (18), in consideration of [2], simplifies to Equation (19) when m = 1 for Rayleigh fading channels.

$$\overline{\gamma}_{EGC} = \left[1 + (L-1)\frac{\pi}{4}\right]\overline{\gamma}$$

( 19 )

## 4. Performance of MQAM in AWGN channel

In this section, the performance of M-QAM over Nakagami-m fading channels is investigated. The SER of square M-QAM (where $\log_2$ M is even) at an instantaneous SNR, $\gamma_k = h^2\frac{E_s}{N_0}$ in an AWGN channel is given by [1]

$$SER_{MQAM} = 4\left(1-\frac{1}{\sqrt{M}}\right)Q\left(\sqrt{\frac{3E_s}{N_0(M-1)}}\right) - 4\left(1-\frac{1}{\sqrt{M}}\right)^2 Q^2\left(\sqrt{\frac{3E_s}{N_0(M-1)}}\right)$$

( 20 )

where $h^2$ embodies the instantaneous power of the fading channel, and h signifies a random variable the channel gain, while $\frac{E_s}{N_0} = \gamma$ indicates the ratio of symbol energy to noise power density in an AWGN channel that is not affected by fading.

For rectangular MQAM (where $\log_2$ M is odd), the SER is tightly bounded by:

$$SER_{MQAM(odd)} \leq 4\left(1-\frac{1}{\sqrt{M}}\right)Q\left(\sqrt{\frac{3E_s}{N_0(M-1)}}\right) - 4\left(1-\frac{1}{\sqrt{M}}\right)^2 Q^2\left(\sqrt{\frac{3E_s}{N_0(M-1)}}\right)$$

( 21 )

By substituting a =$\left(1-\frac{1}{\sqrt{M}}\right)$ and b = $\frac{3}{M-1}$ into Equation (21), it simplifies to:

$$SER_{MQAM} = 4aQ\left(\sqrt{b\gamma}\right) - 4a^2Q^2\left(\sqrt{b\gamma}\right)$$

( 22 )

Q is the Marcum Q-function, and $\left(\sqrt{b\gamma}\right)$ *and* $Q^2\left(\sqrt{b\gamma}\right)$ are defined as [1]

$$Q\left(\sqrt{b\gamma}\right) = \frac{1}{\pi}\int_0^{\frac{\pi}{2}} exp\left(-\frac{b\gamma}{2sin^2\theta}\right)d\theta \quad (23)$$

$$Q^2\left(\sqrt{b\gamma}\right) = \frac{1}{\pi}\int_0^{\frac{\pi}{4}} exp\left(-\frac{b\gamma}{2sin^2\theta}\right)d\theta \quad (24)$$

By numerically solving Equation (23) and Equation (24) using the trapezoidal rule, we get:

$$Q\left(\sqrt{b\gamma}\right) = \frac{1}{2n}\left(\frac{e^{-b\gamma/2}}{2} + \sum_{k=1}^{n-1} e^{-\left(\frac{b\gamma}{2sin^2\left(\frac{k\pi}{2n}\right)}\right)}\right) \quad (25)$$

$$Q^2\left(\sqrt{b\gamma}\right) = \frac{1}{4t}\left(\frac{e^{-b\gamma}}{2} + \sum_{k=1}^{t-1} e^{-\left(\frac{b\gamma}{2sin^2\left(\frac{k\pi}{4t}\right)}\right)}\right) \quad (26)$$

Equation (22) simplifies to;

$$SER_{MQAM} = \frac{a}{t}\left\{\frac{e^{-b\gamma/2}}{2} - \frac{ae^{-b\gamma}}{2} + (1-a)\sum_{i=1}^{t-1} e^{-\frac{b\gamma}{S_i}} + \sum_{i=t}^{2t-1} e^{-b\gamma/S_i}\right\} \quad (27)$$

Where t is the number of summation, $S_i = 2sin^2\theta_i$ and $\theta_i = \frac{i\pi}{4n}$

### 4.1.Performance of MQAM in AWGN channel under Nakagami-m Fading

If $\alpha$ denotes the fading coefficient in a Nakagami-m fading channel, with PDF of $= \alpha^2\frac{E_s}{N_0}$ given by $f_\gamma(\gamma) = \left(\frac{m}{\bar{\gamma}}\right)^m \frac{\gamma^{m-1}}{\Gamma(m)} exp\left(\frac{m\gamma}{\bar{\gamma}}\right)$ [9], then the SER for MQAM is obtained by averaging the SER of the AWGN channel over the PDF of the Nakagami-m fading channel at an instantaneous SNR.

$$P_{ser} = E\left[SER_{MQAM}\right] = \int_0^{\infty} SER_{MQAM}\, f_\gamma(\gamma)d\gamma \quad (28)$$

Where $\bar{\gamma}$-is the average received SNR $\bar{\gamma} = E[\gamma] = E\left[\alpha^2\frac{E_s}{N_0}\right] = E[\alpha^2]\frac{E_s}{N_0}$[11]-[14] Assuming $E[\alpha^2] = \Omega = 1$, then $\bar{\gamma}$=$\frac{E_s}{N_0}$.

Substituting Equation (22) in Equation (28), we get

$$P_{ser} = \int_0^{\infty} \frac{a}{t}\left(\frac{e^{-b\gamma/2}}{2} - \frac{ae^{-b\gamma}}{2} + (1-a)\sum_{i=1}^{t-1} e^{-\frac{b\gamma}{S_i}} + \sum_{i=t}^{2t-1} e^{-b\gamma/S_i}\right)\left(\frac{m}{\bar{\gamma}}\right)^m \frac{\gamma^{m-1}}{\Gamma(m)} exp\left(\frac{m\gamma}{\bar{\gamma}}\right) \mathrm{d}\gamma \quad (29)$$

Equation (29) converges to Equation (30)

$$P_{ser} = \frac{a}{t}\left(\frac{1}{2}\left(\frac{2m}{b\bar{\gamma}+2m}\right)^m - \frac{a}{2}\left(\frac{m}{b\bar{\gamma}+m}\right)^m + (1-a)\sum_{i=1}^{t-1}\left(\frac{mS_i}{b\bar{\gamma}+mS_i}\right)^m + \sum_{i=t}^{2t-1}\left(\frac{mS_i}{b\bar{\gamma}+mS_i}\right)^m\right) \quad (30)$$

The average BER is estimated as [9][10]:

$$P_{ber} \cong \frac{P_{ser}}{k} \quad (31)$$

Where k =$\log_2$M bits/symbol

### 4.2. Diversity Combining with Maximal ratio combining (MRC)

The PDF of the combined instantaneous SNR, under MRC in a Nakagami-m fading channel with L receive antennas, is provided by [4]:

$$f_{\gamma}(\gamma) = \left(\frac{m}{\bar{\gamma}}\right)^{mL} \frac{\boldsymbol{\gamma_i}^{mL-1}}{\Gamma(mL)} exp\left(-\frac{m\gamma}{\bar{\gamma}}\right) \quad (32)$$

Additionally, the SER for MRC is derived by averaging the SER of the AWGN channel over the PDF of MRC in a Nakagami-m fading channel [4,9].

$$P_{ser\_MRC} = E\left[SER_{MQAM}\right] = \int_0^{\infty} SER_{MQAM} f_{\gamma}(\overline{\gamma}) d\gamma$$

$$P_{ser\_MRC} = \int_0^{\infty} \frac{a}{t}\left\{\frac{e^{-b\gamma/2}}{2} - \frac{ae^{-b\gamma}}{2} + (1-a)\sum_{i=1}^{t-1} e^{-\frac{b\gamma}{S_i}} + \sum_{i=t}^{2t-1} e^{-b\gamma/S_i}\right\}\left(\frac{m}{\bar{\gamma}}\right)^{mL} \frac{\gamma^{mL-1}}{\Gamma(mL)} exp\left(-\frac{m\gamma}{\bar{\gamma}}\right) d\gamma \quad (33)$$

Equation (33) can be made to converge by applying the Gamma function property, as stated in [1].

For $\propto > 0$

$$\int_0^{\infty} \gamma^{\propto-1} e^{-\gamma\lambda} d\gamma = \frac{\Gamma(\propto)}{\lambda^{\propto}}, \quad for\ \lambda > 0;$$

( 34 )

By solving Equation (33) using Equation (34), equation (33) becomes

$$P_{ser\_MRC} = \frac{a}{t}\left[\frac{1}{2}\left(\frac{2m}{b\bar{\gamma}+2m}\right)^{mL} - \frac{a}{2}\left(\frac{m}{b\bar{\gamma}+m}\right)^{mL} + (1-a)\sum_{i=1}^{t-1}\left(\frac{mS_i}{b\bar{\gamma}+mS_i}\right)^{mL} + \sum_{i=t}^{2t-1}\left(\frac{mS_i}{b\bar{\gamma}+mS_i}\right)^{mL}\right]$$

( 35 )

From Equation (8), it is clear that the SNR, $\overline{\gamma}_k$, for the channel can be expressed as

$$\overline{\gamma}_k = \epsilon_k E\{\gamma_k\} = \epsilon_k E\left[\alpha_k^2 \frac{E_s}{N_{0k}}\right] = \epsilon_k \overline{\gamma}_{0,c}$$

( 36 )

where $N_{0k}$ signifies the one-sided noise PSD of the $k_{th}$ diversity branch. $\gamma_k$ represents the instantaneous SNR of the $k_{th}$ diversity branch, $\alpha_k$ denotes the instantaneous fading amplitude, and $E_s$ is the average symbol energy.

Consequently, the mean output SNR for each MRC branch is given by:

$$\overline{\gamma}_{k,\,MRC} = \epsilon_k \frac{\overline{\gamma}_{0,MRC}}{L} = \epsilon_k \bar{\gamma}$$

( 37 )

Furthermore, a general expression can be derived for the two common combiners by considering the received average branch SNR, $\bar{\gamma}$. The mean output SNR for each EGC branch can be expressed as:

$$\overline{\gamma}_{k,\,EGC} = \epsilon_k \frac{\overline{\gamma}_{0,EGC}}{L} = \epsilon_k \left(\frac{1 + (L-1)\dfrac{\Gamma^2\left(m+\frac{1}{2}\right)}{m\Gamma^2(m)}}{L}\right)\overline{\gamma}$$

( 38 )

Equations (37) and (38) can be combined to yield:

$$\overline{\gamma}_{0,C} = \epsilon_k \beta_c \bar{\gamma} \tag{39}$$

$$Where\ \beta_c = \begin{cases} \beta_{MRC} = 1\ for\ MRC \\ \beta_{EGC} = \dfrac{1 + (L-1)\dfrac{\Gamma^2\left(m+\frac{1}{2}\right)}{m\Gamma^2(m)}}{L}\ for\ EGC \end{cases}$$

Substituting Equation (39) into Equation (35), where $\overline{\gamma}$ in Equation (35) is equal to $\overline{\gamma}_{0,C}$ when considering a specified combiner, we obtain:

$$P_{ser} = \frac{a}{t}\left[\frac{1}{2}\left(\frac{2m}{b\epsilon_k\beta_c\bar{\gamma}+2m}\right)^{mL} - \frac{a}{2}\left(\frac{m}{b\epsilon_k\beta_c\bar{\gamma}+m}\right)^{mL} + (1-a)\sum_{i=1}^{t-1}\left(\frac{mS_i}{b\epsilon_k\beta_c\bar{\gamma}+mS_i}\right)^{mL} + \sum_{i=t}^{2t-1}\left(\frac{mS_i}{b\epsilon_k\beta_c\bar{\gamma}+mS_i}\right)^{mL}\right] \tag{40}$$

## 5. Results and Discussion

A spatial diversity system for M-QAM modulation in Nakagami-m fading channels was analyzed. It was assumed that all branches have the same average SNR to simplify the analysis. The antenna spacing and fading parameter *m* were varied to examine their effects on correlation. In the figures' legend, "Sim" and "Theory" differentiate between the results from simulations and the analytical model, respectively. The correlation coefficient, ρ, is calculated as described in [17].

$$\boldsymbol{\rho = J_0\left(2\pi\frac{d}{\lambda}\right)} \tag{41}$$

Where $\boldsymbol{J_0}$ is Bessel function of zero order, $\boldsymbol{d}$ is the spacing between antennas and $\boldsymbol{\lambda}$ is the wavelength of the carrier.

The simulation parameters are presented in Table 1, which aligns with Equation (41).

Table 5.1: Simulation Parameters

| $\rho = J_0\left(2\pi\frac{N_r d}{\lambda}\right)$ | $J_0\left(2\pi\frac{d}{\lambda}\right)$ | $J_0\left(2\pi\frac{2d}{\lambda}\right)$ | $J_0\left(2\pi\frac{3d}{\lambda}\right)$ | $J_0\left(2\pi\frac{4d}{\lambda}\right)$ |
|---|---|---|---|---|
| $d = 0.1\ \lambda$ | 0.9037 | 0.6425 | 0.2906 | -0.0550 |
| $d = 0.2\ \lambda$ | 0.6425 | -0.0550 | -0.4020 | -0.1689 |
| $d = 0.5\ \lambda$ | -0.3042 | 0.2203 | -0.1812 | 0.1575 |

For example, if we set the antenna spacing ($d$) to half the wavelength (0.5λ) and choose a specific correlation metric (ρ), and then use a 3-antenna receiving system with equal spacing, we can represent the matrix $\boldsymbol{R}$ in Equation (6) as follows:

$$\boldsymbol{R} = \begin{pmatrix} 1 & -0.3042 & 0.2203 \\ -0.3042 & 1 & -0.3042 \\ 0.2203 & -0.3042 & 1 \end{pmatrix} \tag{42}$$

Furthermore, by applying EVD, we can determine the matrix of eigenvalues corresponding to Equation (42), which is computed using Karhunen-Loève transform (KLT).

$$\boldsymbol{\Lambda} = \begin{pmatrix} 1.5543 & 0 & 0 \\ 0 & 0.7797 & 0 \\ 0 & 0 & 0.6660 \end{pmatrix} \tag{43}$$

$$\rho = J_0\left(2\pi\frac{d}{\lambda}\right) = besselj\left(0, 2\pi\frac{d}{\lambda}n\right) \tag{44}$$

$$\widehat{H} = Q\sqrt{\Lambda}H \tag{45}$$

$$[Q, \Lambda] = svd(R) \tag{46}$$

where $\in_k \in \Lambda$ for Equation (39)

It's noteworthy that the number of iterations, represented by 't' in equation (40), was set to 't = 10'. We found that increasing the iteration count beyond 10 had a negligible effect on the accuracy of the results. This finding was instrumental in selecting the specific value for 't'.

Figures 2 and 3 demonstrate how the error performance varies with the Nakagami-m fading parameter ($m$) for both EGC and MRC using 4-QAM modulation. Considering a diversity order of 3 and antenna spacing of 0.1 wavelengths, we observe that increasing $m$ leads to lower symbol SERs at a given SNR, while decreasing $m$ results in higher SERs. This is because higher $m$ values concentrate the Nakagami-m distribution closer to its mean, mitigating the effects of fading and ensuring signal quality during transmission. As $m$ increases, the channel becomes less prone to errors, improving the SER. Importantly, the simulated and analytical results consistently matched for different $m$ values, including 0.5, 1, 3, and 5.

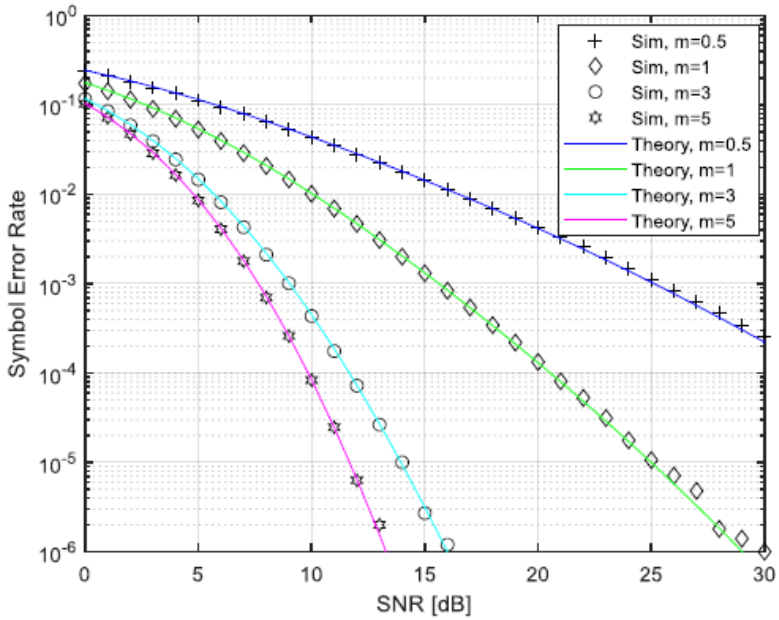


Figure 2: Comparison of Analytical and Simulated Results for EGC with 4-QAM Modulation, $L = 3$, and $d = 0.1\lambda$

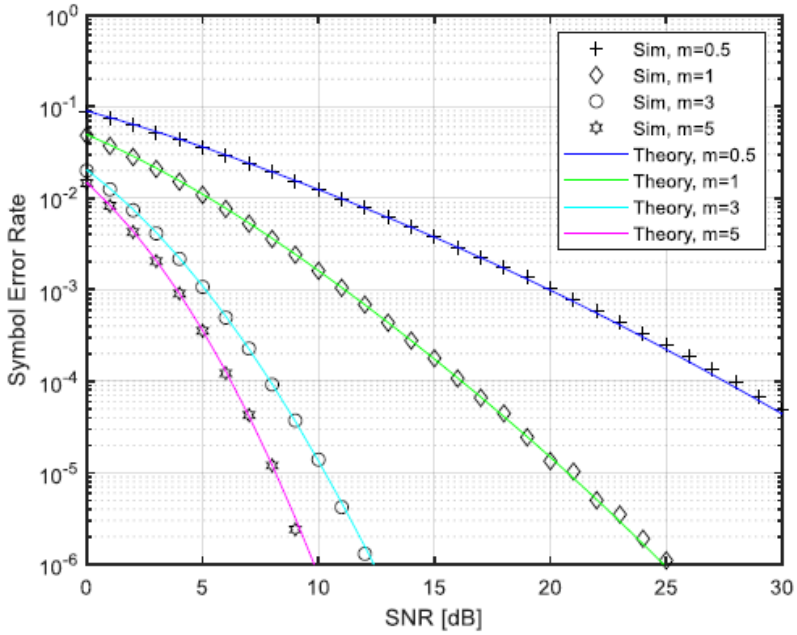


Figure 3: Comparison of Analytical and Simulated Results for MRC with 4-QAM Modulation, $L = 3$, and $d = 0.1\lambda$

Figures 4 and 5 depict the performance of the spatial diversity correlation system for various antenna spacings ($d = 0.1\lambda$, $0.2\lambda$, and $0.5\lambda$) and different fading parameters ($m = 0.5$, 1, 3, and 5) using both MRC and EGC with 4-QAM modulation. A diversity order of 3 was employed. The results indicate that increasing the antenna separation improves the SER. The lowest errors were observed with an antenna spacing of $0.5\lambda$, followed by $0.2\lambda$ and then $0.1\lambda$ for a given

fading parameter m. This is because antennas placed closer together exhibit higher correlation, leading to increased interference between them.

Interference can degrade the received signal, leading to system performance issues. However, increasing the distance between antennas reduces their correlation, resulting in less interference. This can enhance system performance by making the received signal more resilient to interference.

To validate the proposed analytical model, simulations were conducted with various receive diversity branches.

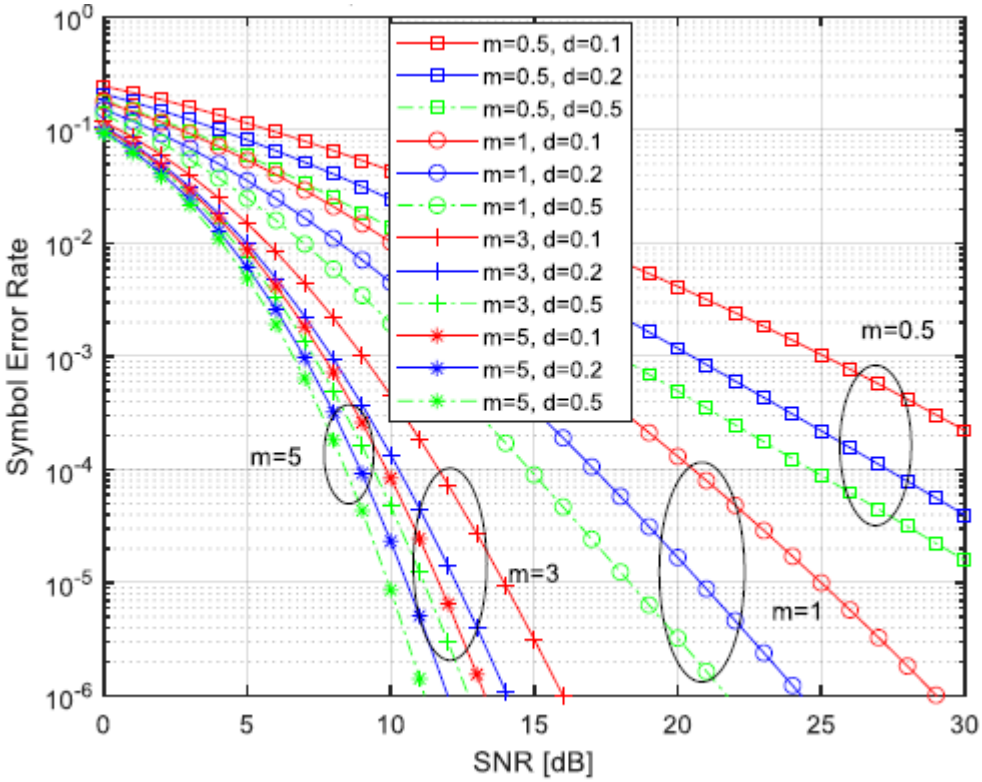


Figure 4: Analytical Results for EGC with 4-QAM Modulation and 3 Correlated Branches ($d$ = 0.1λ, 0.2λ, 0.5λ; $m$ = 0.5, 1, 3, 5)

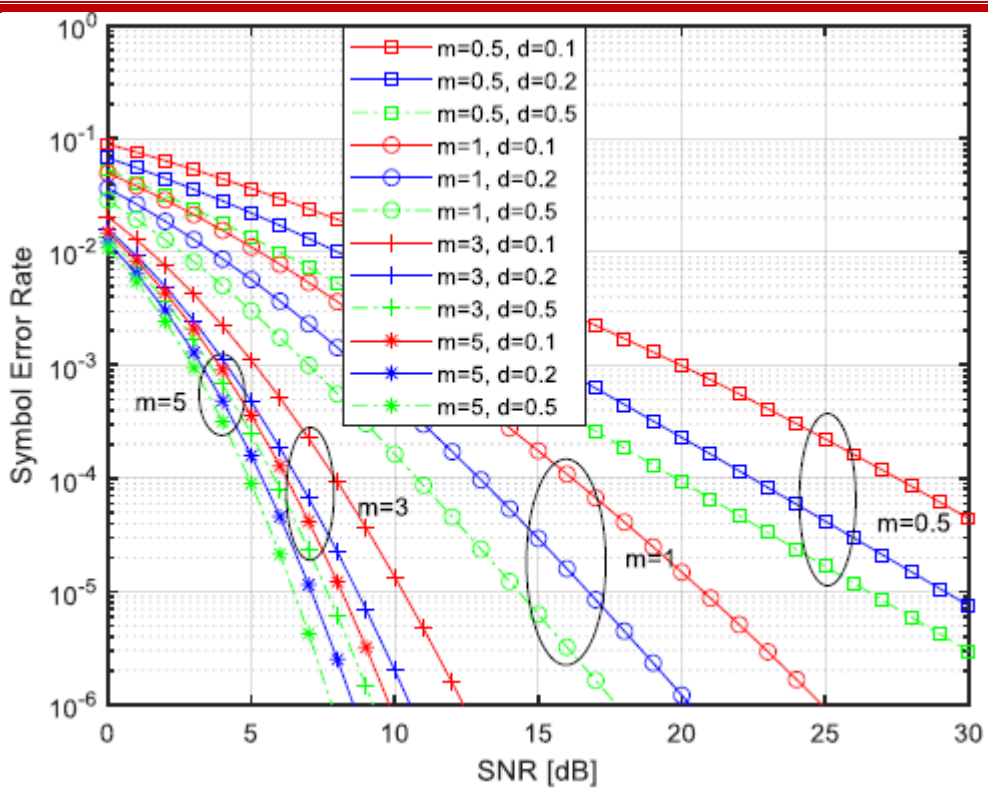


Figure 5: Analytical Results for MRC with 4-QAM Modulation and 3 Correlated Branches ($d$ = 0.1λ, 0.2λ, 0.5λ; $m$ = 0.5, 1, 3, 5)

Figures 6 and 7 present the performance of the spatial diversity correlation system for $L$ = 2, 3, and 4 under both EGC and MRC with 4-QAM modulation. As anticipated, the SER decreased for a given as the diversity order increased. This is because with additional antennas, the system can exploit the spatial diversity of the channel, meaning different antennas receive signals with varying characteristics due to variations in channel conditions.

By combining signals from multiple antennas, the system effectively mitigates the effects of signal fading, improving the overall reliability of the communication channel. This can increase the SNR and reduce the probability of symbol errors. Furthermore, the analytical results closely aligned with the simulation outcomes.

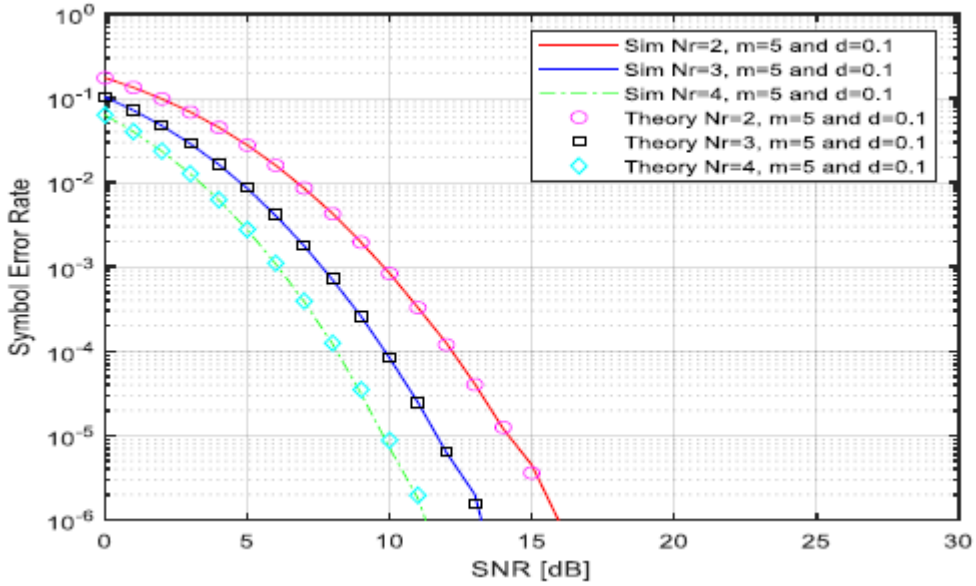


Figure 6: Comparison of Simulated and Analytical Results for EGC with 4-QAM Modulation, $L$ = 2, 3, 4, and $d = 0.1\lambda$

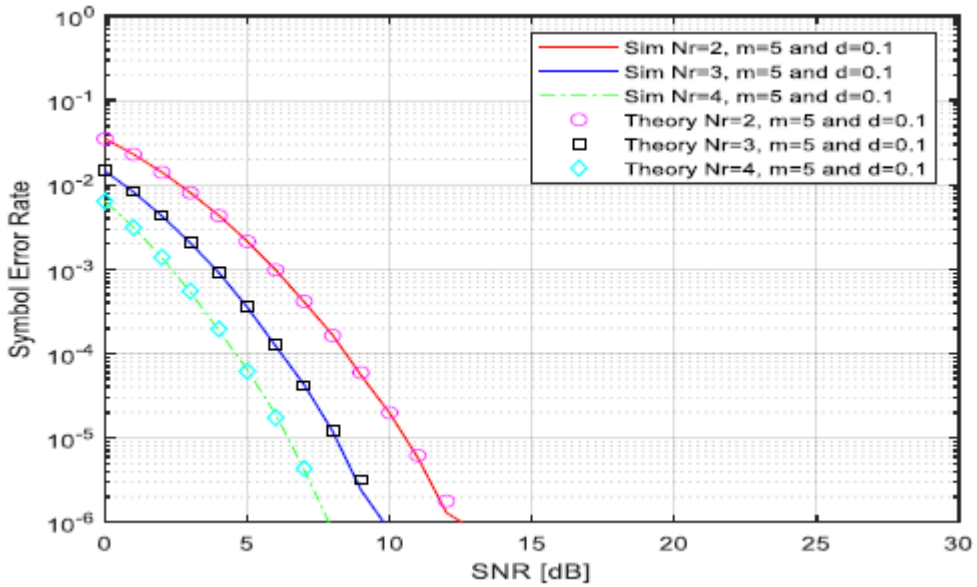


Figure 7: Comparison of Simulated and Analytical Results for MRC with 4-QAM Modulation, $L$ = 2, 3, 4, and $d = 0.1\lambda$

## Conclusion

In this work, a simplified, accurate, and closed-form expression for the SER in correlated Nakagami-m fading channels is derived, which unifies EGC and MRC combining techniques and is applicable across the entire range of SNR values. This unified expression not only reduces computational complexity but also enhances the practical applicability of SER evaluations in multi-branch receive systems. The findings of this study are anticipated to

significantly contribute to the design and analysis of communication systems operating under challenging conditions, thereby advancing the field of wireless communication technologies.

**Future Work**

The existing approximations are not entirely accurate, underscoring the necessity for additional research into deriving exact closed-form expressions for the Q-function. Furthermore, while current studies primarily concentrate on SER performance analysis, there is potential for investigating other metrics, such as secrecy rate. Lastly, a unified SER expression that encompasses MRC, EGC, and SC over Nakagami-m fading channels warrants future exploration.

**Acknowledgment**

We extend our sincere gratitude to the African Development Bank Group (AfDB) for their generous sponsorship of this research. Their support has been instrumental in making this project possible.

Additionally, we would like to express our appreciation to all the individuals and friends we have encountered throughout this research. Their contributions, insights, and encouragement have been invaluable.

**Reference**

1. H. Xu, “Symbol error probability for generalized selection combining reception of m-qam,” South African Institute of Electrical Engineers, vol. 100, no. 3, pp. 68–71, September 2009.
2. J. Lu, T. Tjhung, and C. Chai, “Error Probability Performance of L –Branch Diversity Reception of MQAM in Rayleigh Fading,” IEEE Transactions on Communications, vol. 46, No. 2, pp. 179–181, February 1998.
3. E. Omosa, P. Akuon, H. Xu and O. Kalecha, “Gain of Spatial Diversity with Conjoint Signals in Arbitrarily Correlated Rayleigh Fading Channels,” Hindawi (Wireless Communications and Mobile Computing), vol. 2023, pp. 1–13, November 2023.
4. Al-Shahrani, ‘Performance of MQAM over generalized mobile fading channels using MRC diversity’, M.S. thesis, King Saud University, Riyadh, Saudi Arabia, 2007
5. N. C. Beaulieu, “Pre-processor for receiver antenna diversity,” Patent 08 748 200, December, 2008. [Online]. Available: https://patents.google.com/patent/WO2008144879A1/en
6. E. Omosa, P. Akuon, and O. Kalecha, “Reed-solomon(rs) coding gain on correlated rayleigh fading,” 2019 IEEE AFRICON. IEEE Xplore, July 2020.
7. Karagiannidis, G.K., Zogas, D.A., Kostopoulos, S.A.: ‘Performance analysis of triple selection diversity over exponentially correlated Nakagami-m fading channels’, IEEE Trans. Commun., 2003, 51, pp. 1245–1248
8. Chen, Y.X., Tellambura, C.: ‘Distribution functions of selection combiner output in equally correlated Rayleigh, Rician, and Nakagami-m fading channels’, IEEE Trans. Commun., 2004, 52, pp. 1948–1956

9. D. Rao, Channel Coding Techniques for Wireless Communications, 2nd ed., ser. 2364-6748. Springer Singapore, 2019.
10. Simon, M.K., Alouini, M.S.: 'Digital communication over fading channels' , Wiley-IEEE Press, New York, 2004, 2nd edn.
11. Y.-C. Ko, M.-S. Alouini, and M. K. Simon, "Average SNR of dual selection combining over correlated nakagami-m fading channels," IEEE Communications Letters, vol. 4, no. 1, pp. 12–14, January 2000.
12. Karagiannidis, G.K., Zogas, D.A., Kostopoulos, S.A.: 'BER performance of dual predetection EGC in correlated Nakagami-m fading', IEEE Trans. Commun., 2004, 52, pp. 50–53
13. Sahu, P.R., Chaturvedi, A.K.: 'Performance analysis of predetection EGC in exponentially correlated Nakagami-m fading channel', IEEE Trans. Commun., 2005, 53, pp. 1252–1256
14. Kong, N., Milstein, L.B.: 'Simple closed-form asymptotic symbol error rate of selection combining and its power loss compared to the maximal ratio combining over Nakagami-m fading channels', IEEE Trans. Commun., 2010, 58, (4), pp. 1142–1150
15. Zhou, B., Yang, F., Cheng, J., et al.: 'Performance bounds for diversity receptions over arbitrarily correlated Nakagami-m fading channels', IEEE Trans. Commun., 2016, 15, (1), pp. 699–713
16. Brennan, D.G.: 'Linear diversity combining techniques'. Proc. IRE, 1959, vol. 47, pp. 1075–1102
17. P. Akuon and H. Xu, "Optimal error analysis of receive diversity schemes on arbitrarily correlated rayleigh fading channels," The Institution of Engineering and Technology (IET), vol. 10, no. 7, pp. 854–861, July 2016.
18. R. A. Horn and C. R. Johnson, Matrix Analysis, 2nd ed., ser. 978-0-521-83940-2. One Liberty Plaza, 20th Floor, New York, NY 10006, USA: Cambridge University Press, 2013.
19. E. Omosa, P. Akuon, H. Xu and O. Kalecha, " Characterization of the coding gain for M-PSK with conjoint signals under correlated Nakagami-m fading channels," Springer Open (Journal of Electrical Systems and Information Technology), vol. 10, no. 46, pp. 1–17, October 2023.
20. L. Fang, G. Bi, and A. C. Kot, "New method of performance analysis for diversity reception with correlated rayleigh-fading signals," IEEE Transactions on Vehicular Technology, vol. 49, pp. 1807–1812, September 2000.
21. P. Akuon and H. Xu, "Gain of spatial diversity with conjoint signals." Cape Town, South Africa: AFRICON, 2017 IEEE: IEEE Africon 2017 Proceedings, September 2017, pp.110–114.

# Climate Change and Water Systems Management in Kenya

O. M. Ambani*, E. K. Biamah, C. Kipkemoi

Department of Environmental and Biosystems Engineering, College of Architecture and Engineering, University of Nairobi, P.O. Box 30197, Nairobi-Kenya.

*Corresponding Author: Email: maxwellonzere1@gmail.com

***Article History***
*Submission Date: 8th July 2024*
*Acceptance Date: 10th August 2024*
*Publication Date: 30th September 2024*

## Abstract

Climate change continues to disrupt normal weather patterns in Kenya, causing extreme events like droughts, flooding and heat waves. Currently, the climate change impacts are primarily felt through water. This situation continues to present unpredictable water availability, increased water scarcity and enhanced susceptibility of water supplies to contamination. Furthermore, climate change presents water stress in areas that have limited water resources, which results in increased water completion and conflicts. These impacts continue to drastically affect both the quantity and quality of water needed to sustain people's livelihoods. In the quest for Kenya to get water smart and adapt to water impacts occasioned by climate change, there was an assessment of water-related impacts from climate change and viable water management systems were proposed. This paper examined literature, studies, reports and relevant information regarding water management in Kenya in the wake of climate change. It then looked at the efforts made by the Kenyan government to address water effects such as scarcity and flooding. Finally, existing gaps were identified and addressed through sustainable water management methods proposals, which were grouped into four: conservation systems and practices, allocation methods for water and sewer costs, engagement in retrofit programs, modification of behavioral practices and flood management. An adoption of the proposed strategies is vital towards ensuring that Kenya becomes water SMART with regards to climate change impacts mitigation.

**Keywords**: Climate change, water management, extreme events, water impacts, flood management

## 1. Introduction

Water is an important resource necessary for sustaining livelihoods and contributing to the socio-economic development of countries. In the assumption that there lacked water on earth, life would never exist. For this reason, it is a precious resource that humans need to appreciate and take care of because of its critical applications in agriculture, hydropower generation, manufacturing plants, oil refineries and consumption, among others. The essentiality aspect attached to water means that earth's life depends on it and must therefore, be used sustainably. The finite element of the resource calls for extensive protection and management of water. The resource is under pressure because of its diverse applications in different sectors. Various stakeholders in the water sector continue to appreciate the need of protecting it both at quality and quantity levels, which is why policies continue getting developed to control its usage (Mutschinski and Coles, 2021; Chepyegon and Kamiya, 2018). The development and adoption of water acts is an example of the efforts put in place by different governments globally to protect the resource (Chepyegon and Kamiya, 2018). Therefore, the world appreciates the vitality of the resource and humans are tasked with the responsibility of using it sustainably.

Currently, planet Earth is feeling climate change impacts which continues to disrupt normal livelihoods of people. Water presents a critical resource that is extensively affected and through which the primary climate change effects are felt (Mutschinski and Coles, 2021). An effect on the quantity and quality of water affects human lives that are dependent on it. Some climate change impacts include heat waves, disruption of normal weather patterns, droughts and flooding (Cianconi et al., 2020). The scenario has led to increased water scarcity, unpredictable water availability and susceptibility of water supplies to contamination. High temperature levels catalyze the spread and growth rates of pathogens in freshwater sources, thereby causing a big threat to human health. About 74% of the global natural disasters that took place between 2001 and 2008 were related to water including floods and droughts. With increasing levels of climate change, the expectation is that the frequency shall increase if corrective actions are not taken.

About 43% of Kenya's population does not have access to safe and clean water (Chepyegon and Kamiya, 2018). Water scarcity has been a decade issue in the country that continues to upsurge because of climate change. Some of the attributed causes of the problem include recurring droughts, water contamination and poor management of water supplies (Chepyegon and Kamiya, 2018). Little or no government investments contribute to the water scarcity

problem in rural areas (Chepyegon and Kamiya, 2018). Residents in some urban areas like Mathare and Kibera slums have no option but to use contaminated water, resulting to the emergence of water-borne diseases such as cholera, diarrhea and typhoid (Kim et al., 2022). Another effect that characterizes climate change impact on water is the rising water levels of the Rift Valley Lakes. An example is Lake Nakuru which rose to a height of 8.5m recorded in April, 2020. The results of the rise in water levels include affected ecological life, destruction of water quality, property losses and even deaths. Considering the effects detailed above in the Kenyan context, it can be stated that climate change is here and proper solutions and adaptation strategies need to be adopted. In the quest for Kenya to get water smart and adapt to water impacts occasioned by climate change, it is essential to present strategic solutions regarding viable water management systems. SDG 13 (Climate action), SDG 6 (Clean water and sanitation), SDG 11(Sustainable Cities and Communities), SDG 15 (Life on Land) are few of the goals that need to be addressed in water systems management. The purpose of this work was to uncover the climate change impacts in the Kenyan context and find out the water management strategies that the country has put in place to address the impacts. There is a recommendation on the possible water management strategies that Kenya can adopt for it to become water smart with the looming climate change impacts.

## 2. Climate change in East Africa

The East African region continues to experience negative effects presented by climate change. According to Asokan et al. (2020), projections on climate in the region suggest that there are going to be future extreme and intense events of temperature and rainfall which will affect both the quality and quantity of both groundwater and surface water. The result will be lack of accessibility to clean and safe drinking water, interference with energy resources, food security and health degradation (Luwesi and Di Kayundi, 2019). Most droughts that are experienced in the region are as a result of sporadic and unpredictable rainfall patterns, which has led to areas receiving little or no rainfall in some cases. Lack of rainfall means low moisture levels in soils thereby inhibiting agricultural activities resulting to food insecurity. As at 2019, the region experienced flooding leading to deaths and loss of property. The figure below indicates the reported affected number of people and the number of deaths in the region due to flooding.

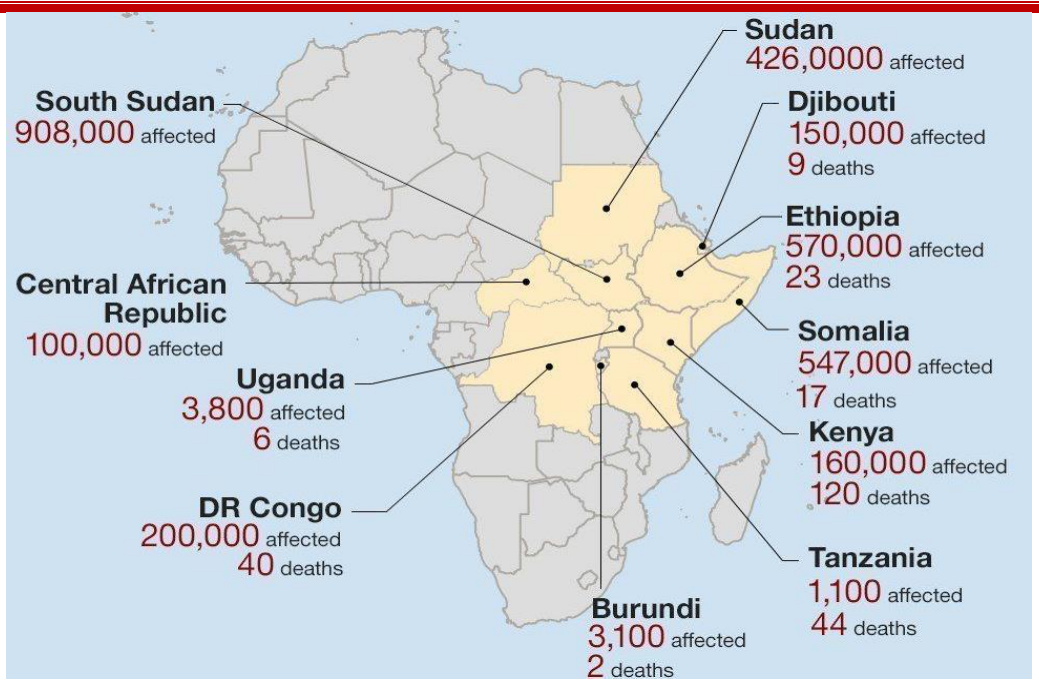


Figure 1: Effects of recent floods in East Africa
Source: (Anon, 2019)

It is important for the countries in the region to have precise knowledge regarding the severity and frequency of the expected extreme events. The knowledge shall help them plan and implement vital implementation to help curb most of the disasters across the region. In doing so, it is important for them tom to stick to the implementation of the water targets laid out by various bodies including Africa Water Vision 2025, African Union Agenda 2063, Kenya Vision 2030, and UN Sustainable Development Goals (Asakon et al., 2020; Mutschinski and Coles, 2021). It is worth appreciating that the region has a lot to do regarding the provision of food security, elimination of poverty and enhancement of healthy living through the adoption of sustainable water management practices.

### 3. Climate change and water management in Kenya

Kenya, one of the biggest economies in East Africa, has continuously experienced extreme events because of climate change. There have been reported droughts, flooding events, disease outbreaks and high temperature levels that have affected agriculture and food security (Kogo et al., 2021). Kenya is greatly susceptible to climate change with projections indicating an annual rise in temperature levels by 2.5$^{o}$C between and 2000-2050. Furthermore, less and intense unpredictable rainfall levels are expected. Any slight increase in drought events will tag along food insecurity and affect water availability, especially in the north and east areas of Kenya known to be arid and semi-arid areas (Kogo et al., 2021).


Figure 2: Drought in Kenya causing death of animals
Source: (Lumosi, 2014)

Approximately 80% of the Kenya's area is either semi-arid or arid with the major economic activity for sustenance of livelihoods being agriculture and pastoralism. Therefore, any negative effect of climate change affects the livelihoods of people which secondarily affects the country's economic growth. Droughts and floods are the key ways through which climate change is exhibited in Kenyan urban areas. An example is the flooding that happens in Nairobi areas like Mathare whenever the city experiences long rains. On the other hand, diminishing water sources indicate the climate change effects in Kenyan rural areas. However, both rural and urban settings in the country are face the challenge of low operating revenues and limited management capacity (Asokan et al., 2021). Limited funding has made it hard to construct or improve water supply systems in areas which suffer from poor or limited water availability.

Despite water not being the only resource affected by climate change in Kenya, it is worth appreciating that it has a critical role regarding adaptation to climate change. Water is solidly linked to other sectors in Kenya including energy and food production (Asokan et al., 2020). Therefore, addressing water issues with reference to climate change will give rise to a holistic approach of building resilience in other sectors. In Kenya, there is a lot of uncertainty attached to the situation including lack of an integrated water management approach, changing climatic conditions, lack of enhanced legislation and implementation of water policies and limited infrastructure (Chepyegon and Kamiya, 2018). It is important for Kenya to develop policies that resonate with addressing water scarcity with regards to climate change. The policies should be in resonance with other global ones since climate change effects on water are felt

both at local and global stages. The country needs to appreciate that the expected increase in water demand occasioned by the increasing population and the unpredictable availability of water because of climate change will force tough decisions to be made regarding water allocation among the different competing users (Asokan et al., 2020).

For Kenya to become water smart and mitigate effects of reduced water availability of water because of climate change, it is important to ensure that there is an efficient and effective participation of all the water stakeholders in the country. Water scarcity can be solved through the implementation of rain water harvesting and storage systems, so that the little available water is captured. The construction of harvesting structures need to be in a way that enhances groundwater recharge to help improve future resilience. Innovative technology regarding sensors, weather forecasts and models are equally important in helping the country avert the effects caused by water problems resulting from climate change.

## 4. Efforts by Kenyan government to address climate change

The Kenyan government has realized the importance of taking measures aimed at addressing the impacts of climate change. At the national level, there is development of a solid regulatory framework made of policies, laws, institutions and plans which are aimed at addressing the issue. Such establishments have been made both at national and county levels. Article 10 of the Kenyan constitution promulgated in 2010 informs the foundation of the legal and institutional frameworks (Kiricho, 2020). It sets out principles like public participation, government devolution and sustainable development which are mandatory when addressing water management systems in Kenya due to climate change. Under article 42, the constitution grants Kenyans the right to a healthy environment which means that even the future generations are entitled to it (Kimkung, 2018). Therefore, the current generation is entitled with the responsibility of protecting the environment to ensure that the future generations enjoy the natural resources currently being enjoyed. From the legal perspective, this entitlement is known as the intergenerational equity principle. Other plans and policies established to combat the effects of climate change include the National Adaptation Plan (2015-2030), National Climate Change Response Strategy (2010), National Climate Change Policy (2018), Climate Risk Management Framework (2017) and Kenya Climate Smart Agriculture Strategy (2017-2026). Another positive note is that Wajir, Makueni and Garissa counties already have an implemented climate change fund regulations that enable them to allocate part of their county budgets towards supporting the local actions to avert climate change.

Kenya has measures in place to reduce on carbon emissions and fast track climate-resilient development that will see it transform to an industrialized middle-income nation. Some of the strategies put in place of reducing carbon emissions include increasing renewable energy proportion to the national grid to 100% by 2030, adoption of sustainable waste management systems, and adoption of climate smart agriculture and promotion of resource and energy efficiency in its different sectors (Okomol et al., 2021. Mungai et al., 2020, Waaswa et al., 2022). Success in the stated aspects will have a positive impact on water availability in Kenya in terms of its quality and quantity. For example, efficient solid waste management systems is likely to lead to improved water quality as the waste that finds way to water bodies will be sustainably contained and managed. Climate smart agriculture has an impact on water quantity as practices such as irrigation will be done effectively when needed and not all the time, which shall help save water usage. Furthermore, reduced carbon emissions into the atmosphere has the merit of Kenya receiving quality rain free from contaminants that arise from carbon's presence in the atmosphere. Therefore, these efforts by the Kenyan government are commendable and their adoption will play a major role in ensuring the country is water smart. There is more to be done to water management, which has not been addressed from the government perspective. The subsequent section proposes efficient, effective and viable solutions to contribute to water management in Kenya.

## 5. Recommended water management methods in Kenya

Considering the current challenges and practices in Kenya regarding water management, there is a need to implement more strategies to help the country be water smart. Increased scarcity of water due to climate change means that business cannot go on as usual since climate change is here with us. It is upon humans, particularly Kenyans in this case to ensure that they engage in sustainable water management practices in the quest to contributing to the SDG 6 on provision of access to clean and safe water for all. The water management systems and strategies are divided into five groups namely: allocation, conservation, behavioral practices, retrofit engagements and flood management (see Figure 3).

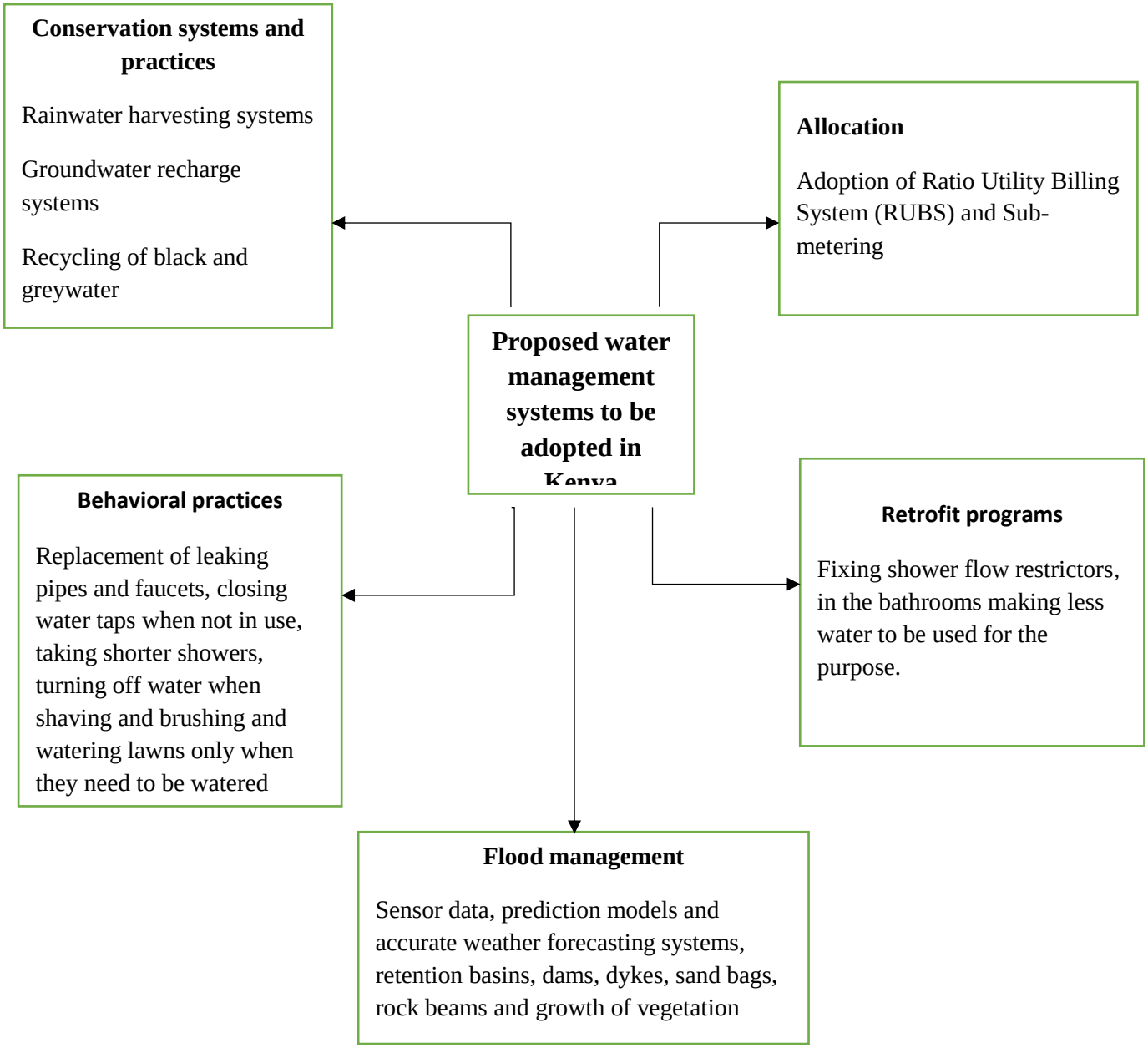


Figure 3: Proposed water management systems in Kenya due to climate change

### i) Conservation systems and practices

The importance attached to water conservation is that it helps in recharging groundwater through the reduction of its consumption as people use alternative water sources. Some of the methods that are applicable in the Kenyan context include:

**Development of rainwater harvesting systems**

Rainwater harvesting systems includes all methods of collecting and storing rainwater for the earth's surface which is received as direct rainfall. The systems are divided into groundwater

recharge where the water is directed to the ground, and rooftop rainwater harvesting that is popular. Rainwater harvesting encompasses the use of simple rain barrels and other elaborate structures made of pumps, tanks and treatment systems. Some of the uses of non-portable water collected using these systems include irrigation of landscaping, washing cars, flushing toilets and even purification for consumption. In Kenya, rainwater collected using rooftop rainwater harvesting systems is often stored in tanks for later use, which is a merit to people since there is lack of assurance on water availability resulting from climate change. However, more adoption of the systems need to be done in other areas as long as they prove viable. Areas such as Makueni, Kitui and regions of North Eastern Kenya receive low rainfall levels. In such areas, practicing rainwater harvesting is critical for its residents to take advantage of the little rainwater available, which can be used during dry seasons and reduce the pressure on municipal systems.

**Groundwater recharge systems**

Most Kenyans abstract groundwater for use, an aspect evidenced by the increased construction of boreholes and collection of water from springs. However, a problem comes in where the volume of abstracted water from aquifers needs to either be less or equal to the volume of recharge. Groundwater recharge makes up part of the processes in the hydrologic cycle where water moves from the earth's surface to the ground, and finally gets stored in an aquifer. Groundwater recharge may either happen naturally because of rain, snowmelt, rivers and lakes or artificially through the infiltration of surface water to the existing shallow aquifers. Groundwater recharge helps increase the volume of water in underground aquifers. Some of the applicable methods in Kenya regarding artificial groundwater recharge include construction of canals across the land surface, using injection wells, adding sprinkler systems and irrigation furrows and constructing infiltration basins. Kenya needs to appreciate these systems to help in groundwater recharge, which shall help in sustainable management of water to reduce in the impact that continue to manifest as a result of climate change.

**Recycling systems for black and greywater**

Greywater refers to the wastewater than emanates from non-toilet stations like baths, showers, washing machines and hand basins. On the other hand, black water refers to water that comes from flushing toilets. It is easy to recycle and reuse greywater compared to blackwater that contains bacteria and viruses responsible for causing diseases. Different methods need to be adopted in Kenya to treat greywater. However, such systems shall depend on the water

characteristics. It is important to note that while adopting the treatment systems, the supply points and pipes containing greywater need to have clear labelling to prevent them from being confused with the ones containing drinking water. For blackwater, there are wastewater treatment plants constructed by the government which are responsible for treating it before discharge. New regulations and policies on release of raw sewage to the environment are being developed and reinforced. Reuse and recycle of both blackwater and wastewater is a rich research area that Kenyan scientists needs to indulge in to provide solutions that shall help meet the increasing water demand. With the increasing effects of climate change, Kenyans need to engage in water recycling and reuse since its availability continues to be threatened by climate change.

### ii) Allocation methods for water and sewer costs

Kenya needs to ensure that every drop of water counts. It is a common practice that for many apartments, especially in the urban areas of the country, the total water bill gets divided by the number of houses and every house pays for the result. There lacks proper mechanisms and systems to ensure that every resident pays exactly for what he/she consumes. This paper proposes two major allocation systems that can be used in the cases of apartments having many residents. These systems include:

**Ratio Utility Billing System**

Under this system, the sewer and water costs in a specific apartment are distributed to every resident with regards to an allocation formula including but not limited to the square footage of a house unit, number of occupants, apartment size, and number of bathrooms, among others. However, the system does not give an exact true cost for every water unit consumed by specific family members. The merit attached to it is that the management of respective apartments are in a position to recapture the utility costs without the need of fixing meters. There is need for landlords to install such systems as they give tenants more incentive with regards to reporting maintenance problems like leaking toilets or faucets. An example of such a system is considering an apartment in Nairobi having 50 occupants and a monthly water bill of Ksh. 50,000. It means that a house having one occupant pays Ksh.1,000. On the other hand, if there is a house with two occupants, they are charged Ksh. 2,000. An adoption of such a system in Kenya shall ensure that people use water sustainably, which a key mitigation measure towards solving the water scarcity puzzle is presented by climate change.

**Sub-metering**

Sub-metering may be used in a case where the house owners want to cut on the overall property consumption. It also presets greater control to residents besides presenting them greater control. Such a system is made of meters used to measure the usage of water for specific units. It also transmits data to a central computer for the purpose of reading and monitoring. Users are able to pay for the specific amount of water that they use instead of paying fixed amounts. The system automatically motivates people to conserve water so that they don't pay huge water bills for misused water. Despite being adopted in some urban areas including Nairobi, Kisumu and Mombasa, it is important to continue adopting it in other areas across the country to help in sustainable use and management of water.

**iii) Behavioral practices**

Behavioral practices calls for the modification of the behavior of people regarding water consumption and usage. It is vital for water to be used efficiently to reduce overall water consumption. However, this recommendation needs to breed from the household level of Kenyans since it is the end point where water consumption takes place. With regards to the modification, awareness needs to be created by all stakeholders in the water sector. Such stakeholders include the Kenyan government, local communities, suppliers, water utility companies, consumers and mangers. Some of the measures that need to be undertaken under the behavioral practices modification include the replacement of leaking pipes and faucets, closing the water taps when not in use, taking shorter showers, turning off water when shaving and brushing and watering lawns only when they need to be watered, among others.

**iv) Retrofit practices**

Retrofit practices include replacing the plumbing equipment under existence with equipment known to consume less water. The advantage attached to these systems is that they are permanent and forms a simple way of conserving water. They can be implemented at little or no costs. However, retrofit equipment are considered effective if they work in the same manner as the old equipment while consuming less water. An example is fixing shower flow restrictors in the bathrooms making less water to be used for the purpose. Both existing and new constructions should be advised to fix low-flow showerheads to help conserve water. It is important for the retrofit programs to include education programs that will help people know here to acquire the low water consuming equipment and their installation methods. Through the adoption of these programs, water will be used sustainably as a mitigation measure to help reduce the pressure on water caused by climate change.

**v) Flood management**

Innovative climate technology such as sensor data, prediction models and accurate weather forecasting systems needs to be adopted and implemented. For example, installation of water level sensors can be helpful in the anticipating flooding events in areas prone to flooding. Their installation on some flooding Rift Valley lakes would have helped in warning people for necessary actions to be taken. Prediction models and accurate weather forecasting systems would have helped in the same case to avoid loss of lives and property. Continuous monitoring of the water levels by using data relayed by the installed systems is of essence.

Other methods that can be applied to avert flooding caused by heavy downpours due to climate change include construction of water retaining structures such as retention basins and dams. In areas where dykes prove viable, they may be constructed to divert the flow of water. Other simple methods include installation of sand bags, rock beams and growth of vegetation to reduce water flow. In urban areas prone to flooding like some parts of Nairobi, there has to be the construction of permeable drainage flows in most courtyards and parking space to enable water to infiltrate into the ground. Maintenance of green areas in the cities is also important to enable the water get reabsorbed into soil. The city storm drains and manholes need to be unclogged to enable free drainage of water that would cause flooding.

## 6. Conclusion

Climate change is herewith the human race and it is upon human beings to take up the mantle and solve the crisis, lest they forget the negative impacts that it causes. Extreme events like prolonged droughts, flooding and upsurge of pests and diseases have characterized Kenya in recent years. The impacts have caused a threat to human sustainability, livelihood and growth. Any threat on human survival means a retarded economic growth level of Kenya. Most of the impacts of climate change are majorly felt through water in different economy sectors. The adoption and implementation of SMART water management systems is key in ensuring that the effects are mitigated. Some of the proposed systems are attainable both at the local and national level. It is upon Kenya and its citizens to ensure that water is managed effectively and efficiently to present sustainability. Every drop needs to count since there is no assurance of water availability. Even if the availability may be assured in cases of flooding, there lacks assurance of its quality. Therefore, both the quality and quantity aspects need to be considered during the implementation of the proposed systems in this paper. Finally, Kenyans cannot afford to wait and actions to avert the current situation need to be taken.

## References

Anon, 2019. How Africa will be affected by climate change. BBC News. Available at https://www.bbc.com/news/world-africa-50726701 [Accessed September 6, 2022)

Lumosi. C. 2014. The Economics of Climate Change in Kenya. Available at https://www.weadapt.org/knowledge-base/economics-of-adaptation/economics-of-climate-change-in-kenya [Accessed January 22, 2024)

Asokan, S. M., Obando, J., Kwena, B. F., & Luwesi, C. N. (2020). Climate Change Adaptation Through Sustainable Water Resources Management in Kenya: Challenges and Opportunities. *African Handbook of Climate Change Adaptation*, 1-11. https://doi.org/10.1007/978-3-030-42091-8_148-1

Cianconi, P., Betrò, S., & Janiri, L. (2020). The impact of climate change on mental health: a systematic descriptive review. *Frontiers in psychiatry*, *11*, 74. https://doi.org/10.3389/fpsyt.2020.00074

Chepyegon, C., & Kamiya, D. (2018). Challenges faced by the Kenya water sector management in improving water supply coverage. *Journal of Water Resource and Protection*, *10*(1), 85-105. https://doi.org/10.4236/jwarp.2018.101006

Kim, J., Hagen, E., Muindi, Z., Mbonglou, G., & Laituri, M. (2022). An examination of water, sanitation, and hygiene (WASH) accessibility and opportunity in urban informal settlements during the COVID-19 pandemic: Evidence from Nairobi, Kenya. *Science of The Total Environment*, *823*, 153398. https://doi.org/10.1016/j.scitotenv.2022.153398

Kimkung, E. L. (2018). *The Right to a Clean and Healthy Environment and the Role of Institutions in Kenya: Steps Forward or Steps Backwards?* (Doctoral dissertation, University of Nairobi). http://hdl.handle.net/11295/105804

Kiricho, J. M. (2020). *The Legal and Institutional Framework for Public Participation in Kenya's System of Devolved Government* (Doctoral dissertation, University of Nairobi). http://erepository.uonbi.ac.ke/handle/11295/154136

Kogo, B. K., Kumar, L., & Koech, R. (2021). Climate change and variability in Kenya: a review of impacts on agriculture and food security. *Environment, Development and Sustainability*, *23*(1), 23-43. https://doi.org/10.1007/s10668-020-00589-1

Luwesi, C. N., & Di Luyundi, T. M. (2019). Quick Appraisal of the Impact of Environmental Changes on Undernutrition in Kenge Health Zone, DRC. *Biomedical Journal of Scientific & Technical Research*, *18*(3), 13529-13536. https://doi.org/10.26717/bjstr.2019.18.003145

Mungai, E. M., Ndiritu, S. W., & Rajwani, T. (2020). Do voluntary environmental management systems improve environmental performance? Evidence from waste management by Kenyan firms. *Journal of Cleaner Production*, *265*, 121636. https://doi.org/10.1016/j.jclepro.2020.121636

Mutschinski, K., & Coles, N. A. (2021). The African Water Vision 2025: its influence on water governance in the development of Africa's water sector, with an emphasis on rural communities in Kenya: a review. *Water Policy*, *23*(4), 838-861. https://doi.org/10.2166/wp.2021.032

Okomol, D. O., Adwek, G., Ngoret, J. K., & Arowo, M. (2021, November). Sustainable Energy Planning Based on the Electrical Grid and Green Energy Transition in Kenya between 2019-2030. In *2021 International Conference on Smart City and Green Energy (ICSCGE)* (pp. 46-51). IEEE. https://doi.org/10.1109/ICSCGE53744.2021.9654364

Waaswa, A., Oywaya Nkurumwa, A., Mwangi Kibe, A., & Ngeno Kipkemoi, J. (2022). Climate-Smart agriculture and potato production in Kenya: review of the determinants of practice. *Climate and Development*, *14*(1), 75-90. https://doi.org/10.1080/17565529.2021.1885336

# The Place of Forensic Structural Audits and Structural Integrity Evaluations in Resolution of Collapsing of Buildings.

S. Murianka[1*] , J. Ireri[2]

[1]Kirinyaga University,P.O. Box 143 - 10300, Kerugoya, Kenya.

[2]Civikraft Engineering, P.O. Box 102068, Nairobi, Kenya. Email:

[*]Corresponding Author: Email: smurianka@kyu.ac.ke

***Article History***
*Submission Date: 31st July 2024*
*Acceptance Date: 25th August 2024*
*Publication Date: 30th September 2024*

## Abstract

Better-quality built structures are in greater demand as a result of public outrage against crumbling buildings and poor construction. Effective management of the building structural integrity inspection process during the construction delivery process and during the building lifetime, maintenance, retrofitting, or expansion is one of the key components of this kind of delivery. This study is a survey of practitioner-completed structural integrity evaluations of projects. The exploratory study aimed to determine the existing state of structural audit procedures and structural integrity assessments through the creation of a standard evaluation approach. The study combines qualitative and quantitative methods, including interviews with important players, observation of buildings in progress, and surveying archives. The results should greatly assist professional organizations and policy makers in rethinking the current structural assessment models in order to attain the affordable housing goals outlined in Kenya Vision 2030.

**Key Words:** construction, structural integrity, forensic auditing, geotechnical.

## 1. Introduction

To begin with, let me clarify that this study is not intended to be a comprehensive treatment of the often discussed topics of structural audits and structural integrity evaluations. It makes more of a suggestion than an explanation. Its goal is to encourage the realization that we are the ones who must lead the way in fostering growth—that is, we must be its creators, overseers, advocates, and leaders. And that "We can, indeed!" It also serves as a kind of synopsis of our

current situation. Where modern thought is leading us, and where fresh developments might take root. The evolution of the structural audit and structural integrity evaluation is then discussed, along with the direction that the more significant trends seem to be taking the paper. The mind is the expert weaver of events. Either ignorance or knowledge can be woven in by us.

In the majority of the world's economies, including the industrialized ones, building failures are frequent. Several historical occurrences have been documented, such as the partial collapse of a parking garage at Eindhoven Airport, the collapse of the Exchange Walkway in Indonesia, the collapse of the Sampoong Department Store in South Korea, the collapse of the Hotel New World in Singapore, and the collapse of the Katowice Trade Hall in Poland. These examples show that building collapse occurs all around the world.

The entire building's health is monitored by structural audits (Gade & Vawhale, 2022). In order to increase the building's appropriateness, safety, and efficiency, it is also necessary to inspect or examine it (Patil & Sayyed, 2015). Structure audits provide information on the building's existing state and the steps that need to be made to extend its lifespan (Gade & Vawhale, 2022). They can also offer suggestions for remodeling and retrofitting. Code rules and standard, recognized techniques for conducting non-destructive testing (NDTs) should be used in the structural audit process.

**Figure 1:** Evaluating the health of a building

The purpose of the structural audit is to keep an eye on the building's general condition and make sure it is safe and risk-free. A structural audit's goal is to identify the components and areas of a building that might require emergency restoration, replacement, or repair. The

structural audits are carried out by qualified experts who are endorsed by government agencies and possess the necessary building industry experience. A structural audit is required by law.

Conducting a structural audit every five years is necessary for structures that are between fifteen and thirty years old. A structural audit needs to be done every three years for buildings older than thirty years. The degree of damage is primarily determined by the caliber of work during the building process. Finding the building's existing state, estimating how long it will last, and identifying any restoration needs in order to extend its lifespan are all crucial. Both financial gains and human lives could be spared by carrying out the structural audits.

The primary obstacle with structural audits is that most experts and the general public are unaware of their value or necessity. First off, according to Gade & Vawhale (2022) one of the aspects of civil engineering that is expanding the fastest is repair and rehabilitation. Second, structural audits make it possible to identify, plan, budget for, and carry out the building's requirements for maintenance, refurbishment, upgrading, and retrofitting. Thirdly, structural audits make it possible to identify the parties at fault when structures collapse. The current system places blame on all construction-related parties, but a structural audit might quickly identify the responsible party. Lastly, when one party believes that neither developer nor contractor has provided value for money, structural audits are utilized to resolve disagreements between the parties. The discrepancy is readily resolved, and the actual worth of the labor completed is established. These are only a few advantages of structural audits that the majority of practitioners are unaware of.

## 2. Literature Review

The majority of nations worldwide have laws that mandate the progressive examination of ongoing construction. It is accomplished in the UK by means of public building inspectors. Nonetheless, several EU nations—most notably Finland, Germany, and Sweden—assign inspection to private companies. This is a recognition of the government's incapacity to gather sufficient funding for such an endeavor.

But having a complex building audit process in place does not ensure perfection. In either case, building failures still happen. Building collapse cases are thoroughly investigated from a criminal perspective, and those responsible for the collapse face punitive measures, such as having to compensate the victims, for their crime or omission. The locations are protected until pertinent research is finished. The majority of the incidents have led to strengthened building control procedures through legislative revisions.

### 2.1. Rehabilitation of buildings

Building rehabilitation entails improving and altering the structure, such as the foundation. The goal of rehabilitation and retrofitting is to reinforce a structure in order to meet the seismic design requirements of the most recent codes. Therefore, it is possible to think of building rehabilitation as a collection of activities intended to raise the standard of building systems in order to comply with functional requirements standards that are more stringent than those that were originally intended. Plastering on walls is typically removed during rehabilitation. Modern, sophisticated treatments for rehabilitation employ a variety of materials, including chemicals, epoxy injection, and other materials.

### 2.2. Structural Audit of Buildings

A structural audit of a building is required in the majority of countries once every three (3) to five (5) years depending on building age. This is carried out in order to verify, using standard values, if the structure is serviceable. In this activity, real information about civil constructions is measured, recorded, observed, and conclusions are drawn. All kinds of technical workers, including contractors and structural auditors, perform audits with essentially the same goals: to ensure that the current structures function as planned. It's critical to understand the building's existing state in order to determine how long it will last or whether repairs are necessary should the structure need to be developed. By recommending preventative and corrective actions like repairs and retrofitting, the structural audit contributes to enhancing the building's life cycle and identifying crucial areas that require attention.

Additionally, structural audits are carried out at different building milestones throughout the process. Since some building projects cannot afford to hire a resident structural engineer, the structural engineers visit the projects on a regular basis while they are under construction. If structural audits are required to confirm that the project is being carried out in accordance with the specifications, they can be carried out whenever the structural engineer thinks it is essential. Depending on the specifics of the contract, the developer, contractor, or structural engineer may be responsible for covering the cost. The project handover milestone, when it could be crucial to verify the quality and craftsmanship prior to the client taking control of the building, is one of these milestones for structural audits.

### 2.3.Structural Audit Process

Understanding the concept and its methodology is the first step in the structural audit process. Second, the rationale behind the structural audit has to be assessed, along with a comprehensive

description of all the necessary characteristics of this kind of audit requirement. Thirdly, an initial survey is conducted to give some idea of the project's actual state. Fourth, the actual created facility is compared to the building blueprints. The next step is a visual inspection to find and record any obvious building code breaches. Critical locations that require testing may now be identified. These will include findings such as water seepage and column and beam cracks (Efendi, 2023).

Tests are then conducted as they are judged necessary. These tests could be both destructive and non-destructive, or they could be both (Assakkaf, 2016). In the event that the tests are inconclusive, more tests can be suggested until a satisfactory degree of assurance regarding the existential problem is achieved. The structural engineer will provide a diagnosis following the delivery of the test findings. The project's structural remediation strategy may be decided upon based on this diagnostic.

## 3. Rationale of the Study

One of the accepted global failures of construction is inadequate research, inadequate investment in research and poor research product uptake. Yet construction exhibits 18 attributes of a chaotic system or a complex system at the very least. It therefore makes sense to make sense of construction through research. The case for structural auditing as an important attribute of the civil engineering and structural engineering industry is full of clarity (Assakfaf, 2016; Ratay, 2000).

The statistics speak for themselves. Mutoro (2011), indicated that 65% of the buildings in Nairobi *are death traps*. According to the Building Audit Report of 2015, the 1980's and early 1990's Kenya had almost zero cases of collapsing buildings (NCA, 2019). Fast track that to three decades later, the sector has been characterized by unsafe buildings that are dangerous for human habitation. Over 100 cases of building collapse have been recorded in Kenya since 1990. An audit by NBI of 14, 895 buildings revealed that 723 are very dangerous, 10,791 are unsafe, 1217 are fair and 2194 are safe. It is estimated that over 200 people have lost their lives since the first building collapsed in 1990, with thousands injured. The economy has equally lost over Kshs 2.4 billion worth of investments.

The case for regulation by civil society is strong. The country is rampant with cases of the civil society taking charge of developmental attributes that the mandated stakeholders have been inept at handling or incapable of reigning in. This is seen in the political arena by the Gen Z and in the legal world by the law society of Kenya. The engineering bodies striving for

relevance and impact will find the same herein. Towards this, NCA (2019) states that the technical capacity of the industry may only be boosted through structured capacity building to grow construction professionals, technicians and artisans in the industry. The study further adds that benchmarking with international best practices would greatly advance local skills for uptake of modern technologies to strengthen the industry's capacity for internal audits to rein on lethargy and corruption (NCA, 2019).

The continuum of progress dictates that a poor idea must always pave way for a good idea, a good idea must pave way for a better idea and the better idea must pave way for the best idea, and further, that the best idea must pave way for the exceptional idea. NCA (2019) admits that there is no policy framework guiding the sector of structural forensic auditing of buildings and the evaluations of building failures. Thus, the nation stands today with a precipice in front and a technological abyss or technological miasma behind. The only logical option is to undertake the steep climb ahead. A third unexplored alternative may exist. The industry could learn to fly. After all Daedalus and Icarus according to Greek mythology were engineers. There is a possibility in the realm of quantum or exponential growth. The complexity of construction has changed in the last three decades. To cope with the current condition, embracing change is imminent. This study posits that the creation of policies and regulations for the expansion of structural audits and structural integrity evaluations into a whole billable consultancy field of its own is such a change.

## 4. Research Methods

The research was designed as a survey targeting structural forensic auditing/structural integrity evaluation projects amongst civil and structural engineering practitioners from a convenient sample of accessible practitioners within Nairobi City County. The sampling unit is also the observation unit which was a project. Roscoe (1975) proposed that sample sizes larger than thirty (30) and less than five hundred (500) are adequate for most researches. The sampling size selected for the survey was fifty (50) projects. A total of fifty (50) questionnaires were sent via email to practitioners. Thirty (30) questionnaires were returned duly completed and all were found to be responsive, representing a 60% response rate. This was deemed appropriate based on Kothari (2004) who opines that a response rate of at least 30% is appropriate. Descriptive statistics were used in the data analysis process. These analyses were carried out using Microsoft Excel.

## 5. Data Analysis and Discussions of Findings.

### 5.1. Source of practitioner training on structural auditing.

The respondents were required to give feedback on the source of their knowledge and training on structural integrity evaluations and forensic auditing. The resulting feedback is provided (Figure 2).

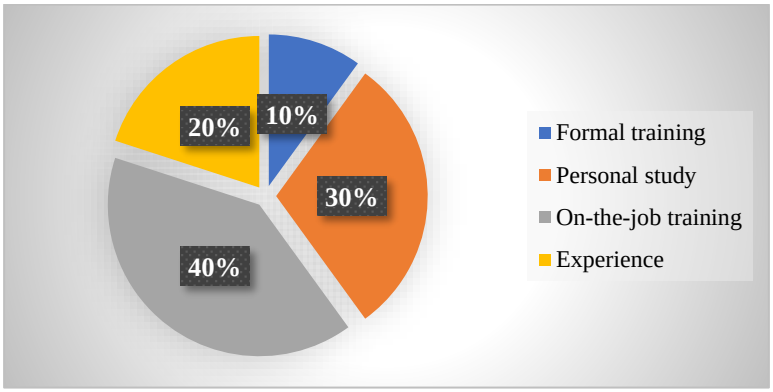


**Figure 2:** Source of practitioner training on structural audits

The highest source of knowledge and training was "on-the-job" training and the lowest was "formal training" at 40% and 10% respectively. Since formal training on the professional skill is a paltry 10%, this indicates a skill gap that construction industry stakeholders like International Labour Organisation (ILO), National Industrial Training Authority (NITA), National Construction Authority (NCA) amongst others may take up to bridge.

### 5.2. Experience of respondents.

There were three (3) categories of experience (Figure 3).The feedback from the practitioners indicated that the highest percentage (50%) of respondents had an experience in excess of ten (10) years while the least percentage (20%) had less than five (5) years' experience.

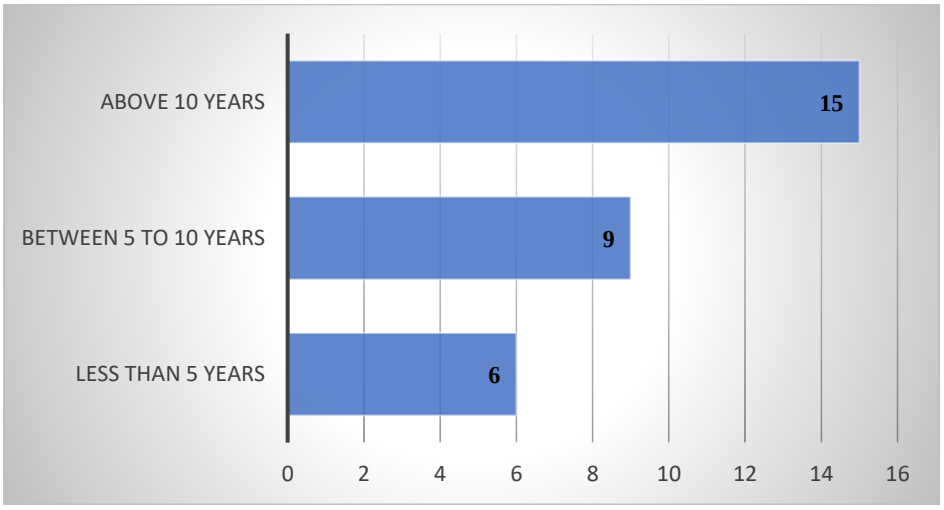


**Figure 3:** Experience of practitioners

### 5.3. Reasons for undertaking the structural audits

The study evaluated the reasons that from which the structural audit or structural integrity evaluation originated. There were five main reasons (Figure 4).

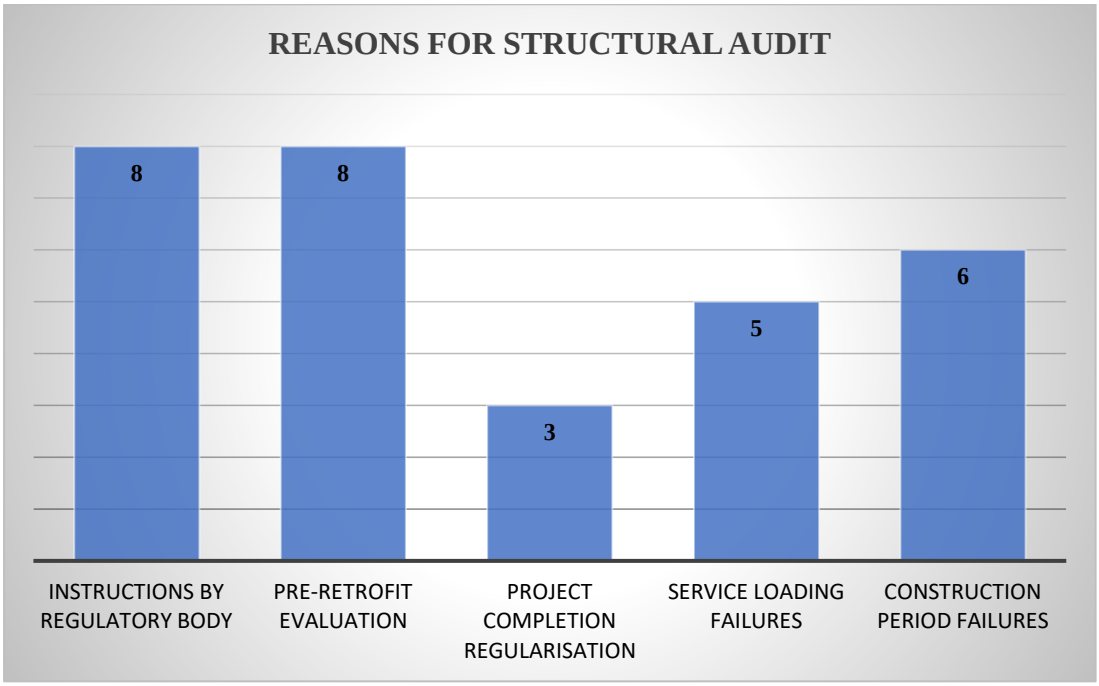


**Figure 4:** Reasons for undertaking the Structural Audit

The most frequent reason for undertaking structural audits was a tie between "instructions from regulatory bodies" e.g. NCA and the County Government and "Pre-retrofit evaluations" both at 27%. Further enquiries pointed out to the fact that inspection by the said authorities pin-pointed to lack of adherence to standards and thus necessitated an evaluation of the constructed works prior to giving the project a clean bill of health and a go-ahead to resumption of works upon temporary stoppage. Moreover, prior to renovating or upgrading an existing facility, a structural audit is mandatory to ensure that the basic assumptions of design for the future alterations are backed by the actuals.

### 5.4. Structural audit tests undertaken on site

Nine categories of tests were undertaken during the structural audits or the structural integrity evaluations (Figure 5).

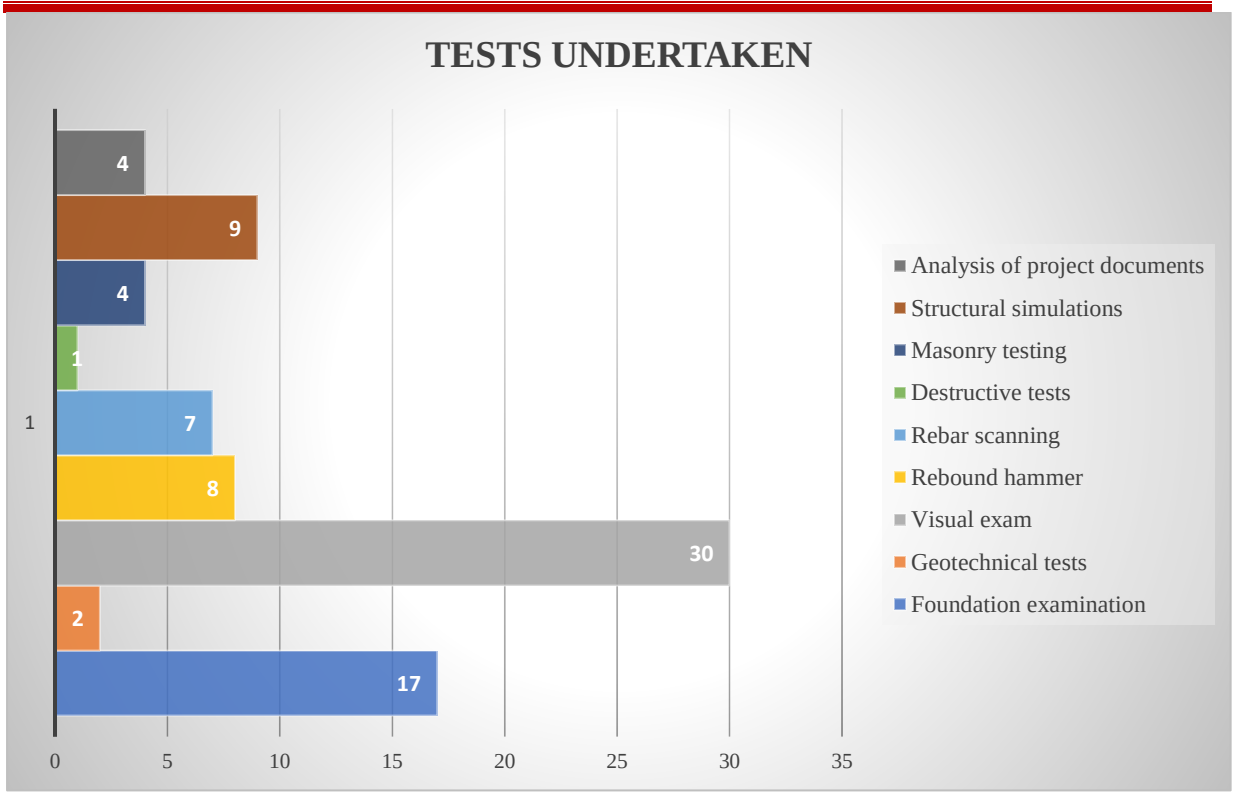


**Figure 5:** Tests undertaken during the structural audits.

Visual examinations were undertaken on all the construction sites or buildings thus this was at 100%. The next highest were "examinations of foundations" on 57% of the projects and "structural simulations" on 30% of the projects. The least number of tests were destructive tests which were only undertaken on one (1) project and geotechnical tests which were undertaken on 2 projects. This is to be expected since geotechnical tests will mostly be undertaken to confirm the nature of the underlying rock when it is determined that the dimensions of the foundation structural elements may not suffice. Moreover, destructive tests are only undertaken when all the non-destructive tests yield unsatisfactory results and it is necessary to conduct a confirmatory destructive test before final diagnosis.

### 5.5. Nature of failures noted during structural audits.

The study also evaluated the main sources of failures in the structural audits or structural integrity evaluations. The failures noted during the structural audits were classified into five (5) categories (Figure 6).

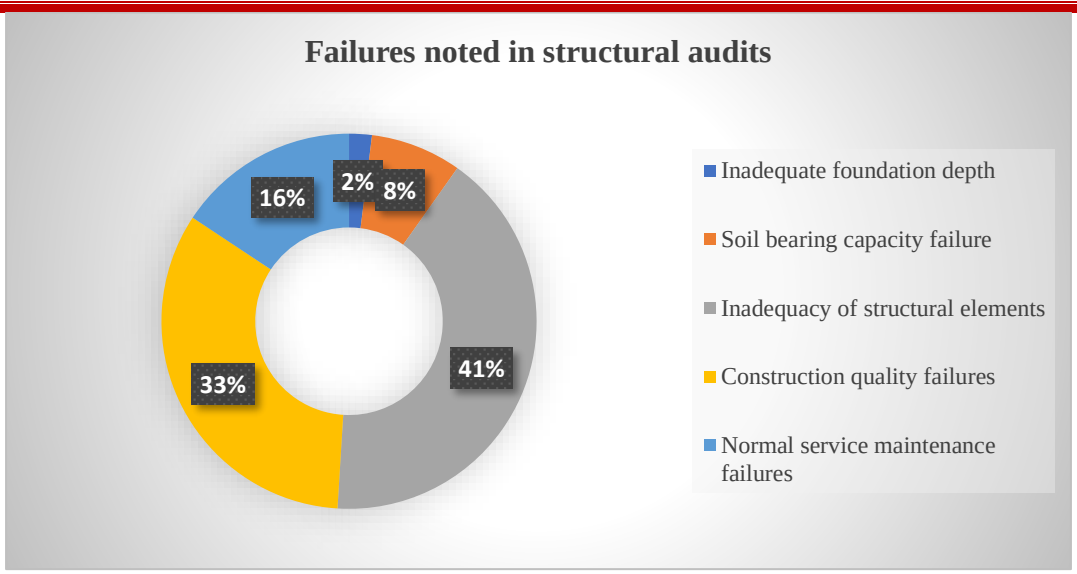


**Figure 6:** Nature of failures noted during the structural audits.

The highest number of structural failures in the projects sampled was "Inadequacy of structural elements" at 41% while the least was "Inadequate foundation depth" at 2%. The structural elements failed in terms of adequacy of structural element sizing, the class or grade of concrete, structural steel size and volume. In some of the projects, the design was at fault while in others the execution was the challenge.

### 5.6. Post-report engagement of practitioners

The study evaluated the percentage of practitioners retained for post-audit supervision where structural remedial works were required for the facility to be given a clean bill of health (Figure 7). A total of seven (7) projects (23%) engaged the structural audit engineer to oversee the structural remedial work while a total of twenty three (23) projects (77%) executed using alternative professionals other than the structural audit engineer.

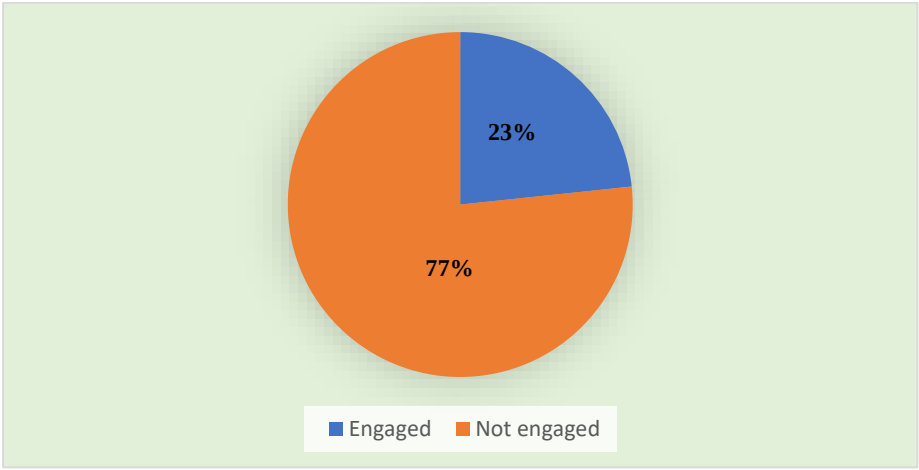


**Figure 7:** Engagement of practitioners after deliver of structural audits.

### 5.7. Structural audit recommendations

The study sought to evaluate the nature of diagnosis upon conclusion of the tests during the structural audits. There were four types of diagnosis recommendations (Figure 8).

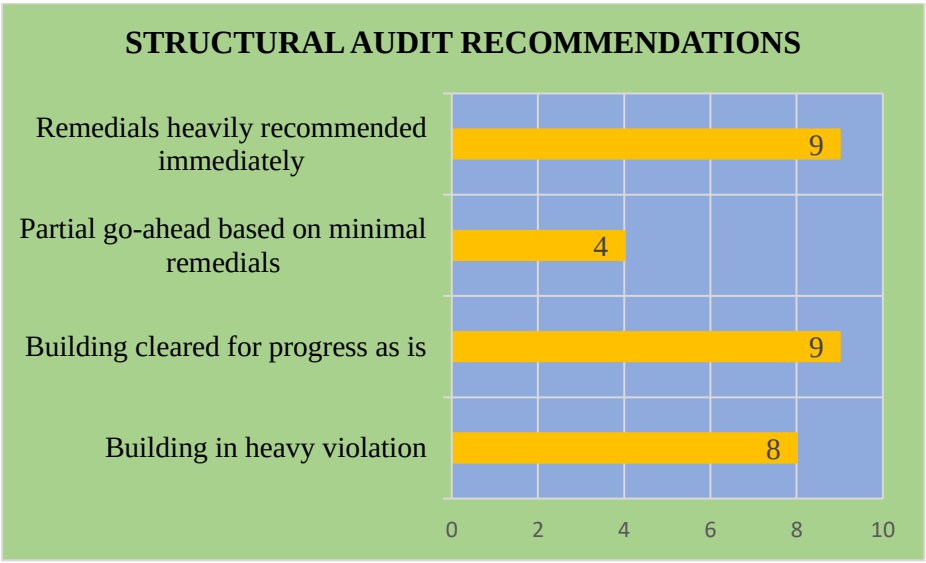


**Figure 8:** Recommendations of the structural audits.

The most frequent recommendations were a tie of "structural remedial works heavily recommended" and "Building cleared for construction progress as is" at nine (9) projects out of thirty (30). The least frequent recommendation was "Partial go-ahead granted based on minimal structural remedial works" in four (4) out of the thirty (30) projects (13%).

### 5.8. Pricing of structural audits.

The general pricing and income generation of structural auditing as a consultancy service was evaluated and the results presented on Table 1 hereafter.

**Table 1:** Analysis of the prices of structural audits

| ITEM | DESCRIPTION | PROJECTS | % BY NUMBER OF PROJECTS | CUMULATIVE SEGMENT INCOME | % BY CUMULATIVE INCOME |
|---|---|---|---|---|---|
| 1. | Below Kshs. 100,000/- | 10 | 33% | 500,000 | 8% |
| 2. | Between Kshs. 100,000 – 250,000/- | 11 | 37% | 1,925,000 | 32% |
| 3. | Between Kshs. 250,000/- to 500,000/- | 7 | 23% | 2,625,000 | 43% |
| 4. | Above Kshs. 500,000/- | 2 | 7% | 1,000,000 | 17% |
| TOTAL | | 30 | 100% | 6,050,000 | 100% |

**Source:** Authors (2024)

From the foregoing, the average cost of a structural audit based on the sampled projects is Kenya shillings two hundred thousand only (Kshs. 200,000.00). From the sample (Figure 9),

37% of the structural audits were priced at between Kshs. 100,000/- to Kshs. 250,000/- representing the highest percentage while the lowest was 2% for structural audits priced at above Kshs. 500,000/-.

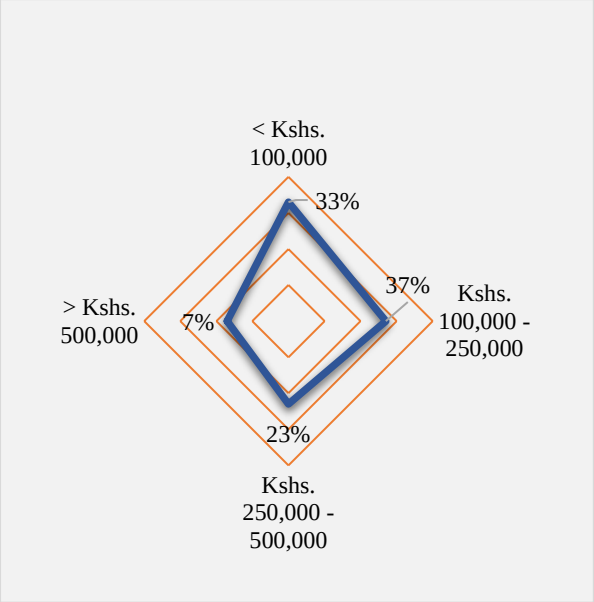


**Figure 9:** Audits by pricing

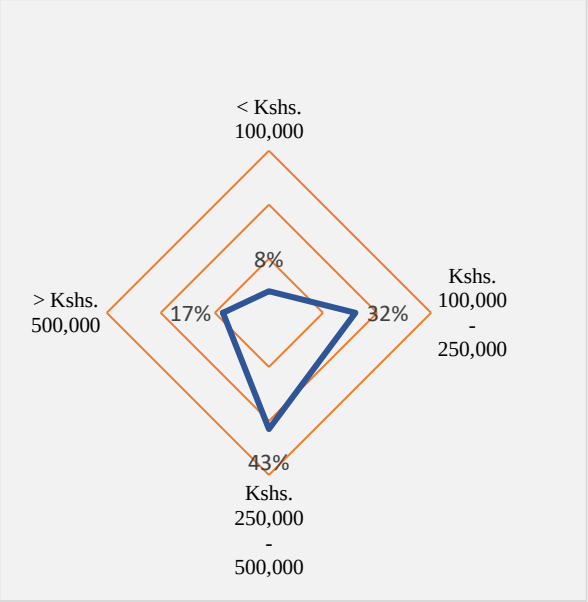


**Figure 10:** Audits by cumulative income

The highest cumulative income generation was achieved by structural audits priced at between Kshs. 250,000/- to Kshs. 500,000/- (43%) while the lowest cumulative income was generated by structural audits priced less than Kshs. 100,000/- (8%).

### 5.9. Cost of structural audits versus cost of building failures

Considering the NCA (2019) statistics that about 100 buildings have collapsed since the 1990s leading to a loss in excess of Kshs. 2.4billion, the average cost of a building collapse is thus at least Kenya shillings twenty four million (Kshs. 24million). Comparing that with the statistics of the previous section that an average audit costs Kshs. 200,000.00 indicates that the cost of a collapse is 120times the cost of an audit or structural integrity evaluation. This, notwithstanding the cost of the 200 stated lives lost through the same in addition to other secondary factors.

## 6. Conclusions and recommendations

The field of structural audits and structural integrity evaluations is critical to the construction industry in Kenya not only for curbing the failure of buildings but also for furtherance of the field of civil and structural engineering. This study concluded that: (i) the policy framework for managing the concept is inadequate; (ii) training gaps exist amongst practitioners; and (ii)

the cost of failure of building is 120 times the cost of structural audits and structural integrity evaluations. As such the following recommendations are made:-

Stakeholders should review the model for management of the attribute within the industry including the certification and generation of standardised pricing schedules.

The engineering bodies, EBK and IEK should evaluate means of bridging the gap in skills and training amongs practitioners.

The construction industry stakeholders should view this and grasp it as an opportunity for broadening the field of consultancy in civil and structural engineering.

**References**

Arya, C. (2009). Design of structural elements: Concrete, steelwork, masonry and timber designs to British Standards and Eurocodes. Taylor & Francis, N.Y., USA.

Assakkaf, I., Sakka, Z. & Qwazeeni, J. (2016). Structural Assessment and Reliability of Existing Building. Asian Pacific Symposium on Structural Reliability and its applications, APSSRA6.

Efendi, A. W. (2023). Identification of Building Reliability with a Forensic Audit of the Non-destructive Test Method. *Jurnal Informasi*, Dan Teknologi, 05(02). E-ISSN: 2829-2758. P-ISSN: 2828-7207.

Gade, L. B. & Vawahle, A. B. (2022) Structural Audit and Rehabilitation of Building. International Research Journal of Engineering and Technology (IRJET), 09(04), 2840-2843. E-ISSN:2395-0056. P-ISSN: 2395-0072.

Mutoro, S. (2011). *Impunity not Judiciary to Blame for Kenya's Collapsing Buildings*. Retrieved July 25, 2012 from http://www.cofek.co.ke

National Construction Authority (2019) Research on Failure and collapse of buildings in the construction industry in Kenya, *National Construction Authority (NCA)*, Nairobi, Kenya.

Patil, S. R. & Sayyed, G. A. (2015). *Structural Audit*. IOSR Journal of Mechanical and Civil Engineering (IOSR-JMCE), 60-64. E-ISSN: 2278-1684.

Ratay, R. T. (2000). Forensic Structural Engineering Handbook. The McGraw Hill Companies Inc., USA.

## Editorial Committee



## Editorial Board



# INSTRUCTIONS TO CONTRIBUTORS

The editorial staff of the AJERI requests contributors of articles for publication to observe the following editorial policy and guidelines accessible at https://www.iekenya.org/ in order to improve communication and to facilitate the editorial process.

## Criteria for Article Selection

Priority in the selection of articles for publication is that the articles:

a. Are written in the English language
b. Are relevant to the application relevant of engineering and technology research and Innovation
c. Have not been previously published elsewhere, or, if previously published are supported by a copyright permission
d. Deals with theoretical, practical and adoptable innovations applicable to engineering and technology
e. Have a 150 to 250 words abstract, preceding the main body of the article
f. The abstract should be followed by a list of 4 to 8 "key Words"
g. Manuscript should be single-spaced under 4,000 words (approximately equivalent to 5-6 pages of A4-size paper)
h. Are supported by authentic sources, references or bibliography

## Rejected/Accepted Articles

a. As a rule, articles that are not chosen for AJERI publication are not returned unless writer (s) asks for their return and are covered with adequate postage stamps. At the earliest time possible, the writer (s) is advised whether the article is rejected or accepted.
b. When an article is accepted and requires revision/modification, the details will be indicated in the return reply from the AJERI Editor, in which case such revision/modification must be completed and returned to AJERI within three months from the date of receipt from the Editorial Staff.
c. Complementary copies: Following the publishing, three successive issues are sent to the author(s)

## Procedure for Submission

a. Articles for publication must be sent to AJERI on the following address:

*The Editor*

*African Journal of Engineering Research and Innovation*

*P.O Box 41346- 00100*

*City Square Nairobi Kenya*

*Tel: +254 (20) 2729326, 0721 729363, (020) 2716922*

*E-mail: editor@iekenya.org*

b. The article must bear the writer (s) name, title/designation, office/organization, nationality and complete mailing address. In addition, contributors with e-mail addresses are requested to forward the same to the Editor for faster communication.

For any queries, authors are requested to contact by mail (editor@iekenya.org).

**PUBLISHER**

The Institution of Engineers of Kenya (IEK)

P.O Box 41346- 00100

City Square Nairobi Kenya

Tel: +254 (20) 2729326, 0721 729363, (020) 2716922

Email: editor@iekenya.org

Website: www.iekenya.org

**CONTENTS**

**Techno-Economic Modelling and Simulation of Offshore Wind Farm for Lamu Port and its Environs ..... 6**

C. B. Owino, G. G. Kidegho, M. J. Saulo

**Enhancing Geothermal Drilling Efficiency: Kenyan Bentonite as a Versatile Drilling Mud.... ……23**

P. M. Weramwanja, G. Rading, T. Ochuku, J. Kihiu, J. Borode

**A Unified Symbol Error Rate (SER) Expression for Equal Gain Combining (EGC) and Maximum Ratio Combining (MRC) over Correlated Nakagami-m Fading Channels..... 37**

E. Omosa, P. O. Akuon, and V. O. Kalecha

**Climate Change and Water Systems Management in Kenya ..... 57**

O. M. Ambani, E. K. Biamah, C. Kipkemoi

**The Place of Forensic Structural Audits and Structural Integrity Evaluations in Resolution of Collapsing of Buildings. ..... 71**

S. Murianka , J. Ireri